Faculty of Physics and Astronomy

Astronomy

University of Heidelberg

Diploma thesis

in Physics

submitted by

Clemens Gneiting

born in Heilbronn, Germany.

2005

HIGGS MASS BOUNDS FROM

RENORMALIZATION FLOW

This diploma thesis has been carried out by

Clemens Gneiting

at the

Institut für Theoretische Physik

under the supervision of

Priv.-Doz. Dr. Holger Gies

Abstract

We use a functional renormalization group equation to determine the renormalization group flow of a Higgs-Yukawa Toy Model mimicking the Standard Model. This approach allows for treating arbitrary bare couplings. We show that for a given ultraviolet cut-off a finite infrared Higgs mass range emerges naturally from the renormalization group flow itself. In agreement with naive expectations, the Higgs mass bounds become more narrow for larger cut-off values. Higgs masses outside the resulting bounds cannot be connected to any conceivable set of bare parameters in the standard-model universality class. For our results, no further physical assumptions have to be imposed, in contrast to many earlier investigations that utilize validity bounds of computational techniques or unphysical instability scenarios.

Zusammenfassung

Wir verwenden eine funktionale Renormierungsgruppengleichung, um den Renormierungsgruppenfluss eines Higgs-Yukawa-Modells zu bestimmen, das das Standardmodell imitieren soll. Dieser Zugang ermöglicht die Betrachtung beliebiger nackter Kopplungen. Wir zeigen, dass sich für einen gegebenen Cut-Off ein endlicher zugänglicher Bereich für die Higgs-Masse im Infraroten als natürliche Konsequenz aus dem Renormierungsgruppenfluss ergibt. Wie naiv erwartet, verengt sich der für die Higgs-Masse zugängliche Bereich mit zunehmendem Cut-Off. Higgs-Massen ausserhalb der resultierenden Schranken lassen sich in der Universalitätsklasse des Standardmodells mit keinem erdenklichen Satz nackter Kopplungen verknüpfen. Im Gegensatz zu vielen vorangegangenen Untersuchungen, die Gültigkeitsgrenzen aus Rechenverfahren oder unphysikalischen Instabilitätsszenarien ableiten, müssen für unsere Ergebnisse keine weiteren physikalischen Annahmen gemacht werden.

Contents

Chapter 1

Introduction

The early twentieth century saw the emergence of the theory of special relativity and quantum theory, describing the physics at high velocities and at small length scales. Provided with the conceptual tools to understand physics in these regions, in the following decades physicists discovered more and more of the (supposedly) fundamental constituents of the world, the so-called elementary particles. The inflationary increase of discovered particles in the fifties and the problems of finding a sensible theoretical description, which were accompanied by confusion and disappointment, could be resolved by a couple of theoretical breakthroughs, which finally resulted in the formulation of the Standard Model. The Standard Model reflects the fact that quantum field theory provides the appropriate language to describe elementary particles, at least at energies accessible at current colliders. The Standard Model not only has proven to be able to describe all experimental data to very high accuracy up to now, but also has brought physicists a huge step closer to their dream of finding a unified theory of all particles and interactions. With the introduction of the Higgs mechanism, all interactions between the fundamental matter fields can be deduced from gauge symmetry. The fermionic matter fields and the weak gauge bosons then acquire their mass through the mechanism of spontaneous symmetry breaking within the Higgs sector involving a fundamental scalar field.

The Standard Model as an effective theory   Despite of its overwhelming success, today the Standard Model is widely believed not to be fundamental. On the one hand, there are arguments of aesthetics: it is considered unsatisfactory that the Standard Model still contains so many parameters

that have to be fixed by experiment. The hope is to find a more fundamental theory that gets by with only very few parameters that have to be set from outside. Second, the Standard Model does not include gravitation. One would expect from a truly fundamental theory to describe all interactions in a unified way.

But, on the other hand, there are also more urging reasons: Already RG-improved perturbation theory suggests that the running couplings of the electroweak interaction and of the scalar self-interaction reach a pole at finite momenta.[1] This is of course no proof of the failure of the Standard Model, since perturbation theory ceases to be a good approximation when a coupling becomes too large, but there are also strong hints from lattice calculations for the existence of these so-called Landau poles, or, more generally, of scales of maximal UV extension [1–3]. We can only escape it by postulating that the Standard Model is not valid up to arbitrarily large momenta, but rather emerges as effective theory from a more fundamental theory, such as string theory.[2] Another way of viewing the same problem is by demanding the Standard Model to be valid up to arbitrarily large momentum scales; one then finds that this is only possible, when the electroweak and scalar couplings vanish in the IR: the theory becomes trivial.

Previous investigations on the range of validity of the Standard Model Ever since it became clear that the Standard Model cannot be valid up to arbitrarily large momentum scales, the question for a quantitative estimate of its range of validity has been raised. When accepting the demand that a fundamental theory should include gravitation in a unified way, an upper bound can be given by the Planck scale, since this is the scale where gravitational effects become of the order of magnitude of the other interactions and therefore cannot be neglected anymore.

It turned out to be possible to deduce much stronger constraints on the threshold of new physics beyond the Standard Model when investigating the scalar sector. The idea is to determine upper and lower bounds on the mass of the not yet discovered Higgs particle by demanding that the scalar effective potential be physically sensible up to a given cut-off scale. Thus,

---

[1]The strong interaction on the other hand is known to be asymptotic free, therefore allowing for a save completion in the UV.

[2]Actually there is one loophole left: One might think of the scenario that there exists a non-Gaussian UV fixed point of the Standard Model, allowing for a save route to the UV. This has indeed been investigated [4].

the experimental verification of the existence of the Higgs particle and the knowledge of its mass would make it possible to give an explicit estimate of the cut-off, which might be much closer to the IR than the one mentioned above. On the other hand, these bounds can tell us where we have to expect the Higgs mass, at all. The upper bound to the Higgs mass at a given cut-off is deduced from the Landau pole; it is clear that a theory which exhibits a Landau pole is not defined beyond the pole. Hence, the scale of the pole yields an estimate of the cut-off. So far, the investigation of the Landau pole is based on RG-improved perturbation theory and lattice calculations [5–7]. Actually, only the latter is capable of exploring the non-perturbative regime. Treating this issue with other, more appropriate non-perturbative methods appears urgent.

The lower bound originally was derived from the requirement that the scalar effective potential be stable or at least meta-stable up to the threshold of new physics [8–18]. This approach to the lower bound was recently put into question by Holland [19] and by Branchina and Faivre [20]. In order to illustrate the original line of arguments, we restrict us to a simple Higgs-Yukawa model of a single real scalar field coupled to one Dirac fermion field, which stands for the Top quark. In the next chapter, we will argue that this model is indeed an acceptable first approximation to the Standard Model when focusing on the radiative corrections to the scalar effective potential. It should at least reproduce qualitatively the effects on the full Standard Model scalar effective potential.

Let us summarize the conventional line of argument. The seeming problem can already be seen in a straightforward one-loop mean field calculation of the scalar effective potential. The effective potential then reads

$$
\begin{aligned}
U_{\text{eff}} &= V + 1/2 \int_k \ln\left[k^2 + V''\right] - 2 \int_k \ln\left[k^2 + h^2\,\phi^2\right], \\
V &= \frac{m^2}{2}\,\phi^2 + \frac{\lambda}{24}\,\phi^4.
\end{aligned}
$$

V denotes the classical scalar potential, h the Yukawa coupling. The fermion contribution is negative due to the minus sign associated with every fermion loop. Regulating the integrals and adding counterterms to absorb the divergences in the normal fashion ($\overline{MS}$ scheme), the renormalized effective

potential is given by

$$U_{\text{eff}} = V + \frac{(V'')^2}{64\,\pi^2}\left\{\ln\left[\frac{V''}{\mu^2}\right] - \frac{3}{2}\right\} \qquad (1.1)$$
$$- \frac{h^4\,\phi^4}{16\,\pi^2}\left\{\ln\left[\frac{h^2\,\phi^2}{\mu^2}\right] - \frac{3}{2}\right\},$$

where μ denotes the renormalization scale. One sees easily that, according to (1.1), the negative fermion contribution dominates for large ϕ, if $\lambda^2 < 16\,h^4$. In this case, at some point the potential bends down and runs towards $-\infty$. In the best case, this just means that our electroweak minumum is not the absolute minimum, and the vacuum sooner or later tunnels into its true vacuum (given new physics prevents the potential from growing ever more negative). In the worst case, taking (1.1) literally, this means that our theory is sick, since there is no vacuum. We get a cut-off estimate by demanding that new physics prevents the potential from becoming smaller than the electroweak minimum, at all. Thus, the effective theory can only be valid up to the scale, where the potential passes the depth of the electroweak minimum. On the other hand, when we require the potential (1.1) to be stable without introducing new physics, which corresponds to $\lambda^2 > 16\,h^4$, we get for a fixed Yukawa coupling h a lower bound for λ and hence for the Higgs mass (at tree level the relation is $\lambda = 3\,m_{\text{Higgs}}^2/v^2$). Of course, since (1.1) is just a one-loop calculation, it is not trustworthy for large ϕ due to the large logs, even when the couplings are small. But it turned out that RG-improved two-loop calculations in the Standard Model also suggest the appearance of the instability [15, 17].

As mentioned above, recently the existence of the instability at all was put into question. K. Holland investigated the Higgs-Yukawa model on the lattice (which corresponds to a cut-off theory) and did not find any instability [19]. The author argues that the instability is a spurious leftover of the incorrect sending of the cut-off to infinity; the standard renormalization procedure of adding counter terms and removing the cut-off would fail in a trivial theory. Only for a finite cut-off a trivial theory can have a non-trivial interaction. He shows that the one-loop effective potential with counter terms added does not exhibit the instability as long as the cut-off is kept finite.

Branchina and Faivre, on the other hand, argue that the instability occurs in a region of ϕ, where the renormalized potential is not valid anymore. In detail, they start with the bare one-loop effective potential of the Higgs-Yukawa

7

Model with a cut-off and show that it is – independently of the bare parameters – stable in the region where it is defined, $\phi < \Lambda$. Then they reformulate it in renormalized quantities. The resulting potential, which shows the instability for certain choices of the renormalized parameters, is commonly believed to be a trustworthy approximation as long as the renormalized couplings are perturbative,

$$\lambda_\mu \ll 1 \qquad , \qquad h_\mu \ll 1, \qquad (1.2)$$

and the leading log is still small,[3]

$$\left| \frac{h^4}{16\,\pi^2} \ln \frac{\phi^2}{\mu^2} \right| \ll 1. \qquad (1.3)$$

But the authors explicitly construct a $\overline{\phi}$ that on the one hand fulfills (1.2) and (1.3), but on the other hand also yields

$$\overline{\phi} \gtrsim \Lambda,$$

which means that it is situated beyond the region of validity of the potential.[4] They deduce that the requirement of (1.2) and (1.3) is not sufficient to guarantee the validity of the approximation, but should be completed by the additional condition[5]

$$\frac{\lambda_\mu}{24}\,\phi^4 + \frac{h^4\,\phi^4}{16\,\pi^2} \ln \frac{\mu^2}{\phi^2} > 0.$$

They show that, when respecting this additional condition, no instability occurs. Physically, this new condition can be attributed to the fact that the renormalized couplings cannot be chosen freely, since they emerge from the bare couplings. Branchina and Faivre then derive a new criterion for the determination of the cut-off by arguing that new physics has to set in at the inflection point of the potential. However, this criterion is somewhat arbitrary; the inflection point only marks the breakdown of the approximation, not necessarily the onset of new physics.

---

[3]If we assume the renormalized parameters to be chosen such that the instability occurs, we can neglect the scalar fluctuations, since then they do not influence the situation qualitatively.

[4]We will give a more detailed description of this line of argument in Chapter 7 for the simple example of the fermionically induced scalar effective potential.

[5]The scale dependence of h is neglected.

Our approach   We also consider the Higgs-Yukawa Toy Model. We expect that for arbitrarily chosen (physically sensible) bare couplings at a given cut-off the theory only allows for a finite range of renormalized couplings, which again yields a finite range of possible Higgs masses. Thus, we do not employ any kind of physical condition as indicator for the onset of new physics, but rather ask which Higgs masses are possible at all for a given cut-off. We face a naturally non-perturbative problem, since we have to probe arbitrarily large bare couplings. We deal with this situation by applying an exact renormalization group equation. By scanning the parameter space at a given cut-off and determining the resulting renormalized couplings, which then allow for the calculation of the Higgs mass, we intend to constrict the allowed range of Higgs masses.[6] A measurement of the Higgs mass then would allow for an estimate of the maximum scale of validity of the Standard Model.

Outline   In the second chapter we argue that the Higgs-Yukawa Toy Model is indeed a qualitatively reasonable approximation to the Standard Model when focusing on the scalar effective potential, which finally sets the Higgs mass. In chapter three we introduce the renormalization group idea and derive the exact renormalization group flow equation that we use in our approach. In the fourth chapter we motivate a truncation of the Toy Model effective action and derive the resulting flow equations from our exact renormalization group flow equation. The fifth chapter deals with our way of numerically implementing the previously derived flow equations. While chapter six is dedicated to some benchmark tests of our numerical approach, in the seventh chapter we finally investigate the issue on the Higgs mass constraint. We conclude this work with a summary and an outlook to possible further investigations.

---

[6] The parameters at the cut-off are constrained by the requirement that the renormalized fermion mass and the resulting vacuum expectation value have to match the experimental values.

Chapter 2

From the Standard Model to our Toy Model

In this chapter we want to motivate that the Higgs-Yukawa Toy Model we investigate is indeed a qualitatively reasonable approximation to the Standard Model with respect to the properties of our interest, namely the scalar effective potential and the resulting Higgs mass. We remind the reader that this model consists of one real scalar field and one Dirac spinor field, which stand for the Higgs particle and the top quark, respectively. The scalar field exhibits an arbitrary self-interaction. Both fields are coupled through a Yukawa interaction.

We proceed in two steps: First we argue that the only dominant influence of the other sectors on the scalar sector is through the top quark; second, we motivate that the scalar sector itself can be reduced to a real scalar field with a discrete symmetry.

Influence of the other sectors on the scalar sector We begin by realizing that most sectors of the Standard Model are experimentally probed to be in the perturbative regime at low energies;[1] only the scalar sector might turn out to be non-perturbative. Even the Yukawa couplings have to be perturbative in the IR, which can easily be derived when taking the SM best fit

---

[1]We are aware that the strong interaction becomes highly non-perturbative in the IR; but this occurs only at very low energies, far below the scale of electroweak symmetry breaking. We therefore take the viewpoint that the IR evolution of the strongly interacting sector does not have a significant influence on the scalar effective potential, since its flow should have already frozen out by then.

result for the vacuum expectation value from high precision measurements into account.[2] We therefore can follow a perturbative line of argument and give the effective potential in terms of a loop expansion. The effective potential is the sum of all 1PI graphs with vanishing external momenta (more detailed: the nth derivative of V is the sum of all 1PI graphs with n vanishing external momenta). The corresponding calculation has been done for the Standard Model to high accuracy, RG improved up to two-loop order [13, 15–17]. For our reasoning it is sufficient to consider the one-loop result, which reads in the 't Hooft-Landau gauge and the $\overline{MS}$ scheme

$$
\begin{aligned}
V &= V_0 + V_1 \\
&= -\frac{1}{2}m^2(t)\,\phi^2(t) + \frac{1}{8}\,\lambda(t)\,\phi^4(t) \\
&\quad + \sum_{i=1}^{5} \frac{n_i}{64\,\pi^2}\,M_i^4(\phi)\left[\log\frac{M_i^2(\phi)}{\mu^2(t)} - c_i\right] + \Omega(t),
\end{aligned}
\tag{2.1}
$$

with

$$
M_i^2(\phi) = \kappa_i\,\phi^2(t) - \kappa_i'
$$

and

$$
n_1 = 6, \qquad \kappa_1 = \tfrac{1}{4}g^2(t), \qquad \kappa_1' = 0, \qquad c_1 = \tfrac{5}{6};
$$

$$
n_2 = 3, \qquad \kappa_2 = \tfrac{1}{4}\left[g^2(t) + g'^2(t)\right], \qquad \kappa_2' = 0, \qquad c_2 = \tfrac{5}{6};
$$

$$
n_3 = -12, \qquad \kappa_3 = \tfrac{1}{2}h_t^2(t), \qquad \kappa_3' = 0, \qquad c_3 = \tfrac{3}{2};
$$

$$
n_4 = 1, \qquad \kappa_4 = \tfrac{3}{2}\,\lambda(t), \qquad \kappa_4' = m^2(t), \quad c_4 = \tfrac{3}{2};
$$

$$
n_5 = 3, \qquad \kappa_5 = \tfrac{1}{2}\,\lambda(t), \qquad \kappa_5' = m^2(t), \quad c_5 = \tfrac{3}{2}.
$$

$\Omega(t)$ is the one-loop contribution to the cosmological constant, which will play no role in our investigations.[3] $m(t)$ and $\lambda(t)$ are the quartic coupling and mass of the scalar field(s),[4] whereas $g(t)$, $g'(t)$ and $h_t(t)$ are the SU(2)

---

[2]Only the top-Yukawa coupling may be viewed as being at the brink of the perturbative validity domain. For $m_t = v\,h_t$, $m_t = 178\,\mathrm{GeV}$ and $v = 247\,\mathrm{GeV}$, we get $h_t = 0.72$, which is only slightly smaller than 1.

[3]Actually, we will even get rid of it by explicitly subtracting any offset at $\phi = 0$.

[4]The SM scalar sector consists of an isospinor of two complex fields; but due to symmetry, they have the same masses and couplings. By exploiting the gauge symmetry, (2.1) could be written as a function of a single field ϕ.

gauge coupling, the U(1) gauge coupling and the top quark Yukawa coupling, respectively. Among the Yukawa couplings the top quark Yukawa coupling has to be by far the largest, since the Yukawa couplings are directly connected to the fermion masses. That is why we have in a first step already neglected in (2.1) the Yukawa couplings of all the other fermions with smaller masses; their contributions are small compared to the contribution of the top quark. But the same is true for the gauge couplings $g(t)$ and $g'(t)$: in the IR they are known to be much smaller than the top Yukawa coupling and the SU(3) gauge coupling. And despite of their growing with increasing momentum, they remain smaller at least up to the GUT scale, where they intersect with the running SU(3) coupling g_3. Thus, we can also neglect the contributions from the electroweak interaction to the scalar effective potential (and to the β functions of the remaining couplings), which corresponds to leaving out $i = 1, 2$ in (2.1). At this point, the only connection left to the other sectors of the SM is via the top Yukawa interaction. Before we restrict us to the top quark alone, we first check if the neglected components of the SM make significants contributions to the flow of the top Yukawa coupling. By inspection of the one-loop β function of the top Yukawa coupling [13],

$$\beta_{h_t}^{(1)} = \frac{1}{16\,\pi^2} \left(\frac{9}{2} h_t^3 - 8\,g_3^2\,h_t - \frac{9}{4}\,g^2\,h_t - \frac{17}{12}\,g'^2\,h_t \right),$$

we indeed find that the SU(3) gauge coupling g_3 makes a significant contribution to the flow: for $\alpha_s = g_3^2/4\,\pi = 0.118$ and $h_t = 0.72$, we get $8\,g_3^2\,h_t = 8.52$, whereas $\frac{9}{2}\,h_t^3 = 1.68$ (the weak couplings g and g' are negligible, as mentioned above). In a full quantitative treatment, we would have to take it into account. But since we are only interested in the gross qualitative properties of the scalar effective potential, we can safely omit this influence of the strong interaction; we do not have to expect any surprising effects on the scalar potential from it. Due to the asymptotic freedom of the strong interaction, this contribution becomes smaller with larger momenta, anyway.

Modelling the scalar sector So far, we have boiled the SM down to the scalar sector coupled to the top quark. If we want to end up at our Toy Model, we still have to simplify the scalar sector itself. Actually, by neglecting the electroweak interaction, we spoiled the original gauge invariance of the scalar sector. But without gauge invariance and the gauge bosons, we are left with a mere global invariance of the scalar isospinor Lagrangian. It is

clear that we cannot leave it at this: spontaneous symmetry breaking in a theory with global continuous symmetry inevitably results in the occurence of Goldstone bosons, which we do not want, since in the SM they are "eaten" by the gauge bosons. In the case of the full SM, we saw that it is possible to write the scalar potential as function of just one scalar field by exploiting the gauge invariance. Thus, without gauge invariance, we just approximate the scalar sector by a single real scalar field right from the start. Since a theory of a single scalar field does not exhibit a continuous symmetry, we avoid the occurrence of Goldstone bosons. Hence, the nature of the degrees of freedom corresponds to that of the SM. The original SU(2) symmetry then is modeled by a discrete symmetry (Z_2). The symmetry is needed to restrict the allowed spectrum of operators in the effective potential and to simulate chiral invariance inhibiting direct fermion masses. It turns out that the demand of parity in the case of a single scalar field suffices to simulate the restrictions of the SU(2) symmetry on the scalar potential in the SM case.

One loophole left ...   The argumentation above is strongly relying on the perturbativity of all sectors of the SM. We only can be sure that our Toy Model is a valid approximation to the SM as long as this requirement is given. As mentioned above, we can indeed assume the SM to remain perturbative up to the GUT scale, but only if the scalar sector itself remains perturbative and thus controllable throughout all scales in between. Now a major point of our investigation will be explicitely to allow for large couplings; we want to probe the whole parameter space of bare couplings of our Toy Model. We have to expect that a highly non-perturbative scalar sector also has strong effects on the flow of all the other sectors – they might even be driven non-perturbative, as well –, which in turn might have a non-negligible backlash on the scalar sector itself; the disregard of the other components besides the top quark would not be justified anymore. On the other hand, if strong dynamics play a role in the SM in the UV, its qualitative mechanisms may already be visible in its Toy-model counterpart.

Chapter 3

The renormalization group method

We formulate our Toy Model as a functional integral up to some maximum momentum scale, the cut-off. The introduction of the cut-off is motivated by the fact that the Standard Model cannot be valid up to arbitrarily large momentum scales, anyway, and therefore should be understood as effective theory. The functional integral formulation yields a beautiful intuitive picture of the meaning of fluctuations, since it makes manifest that the field is not constricted to the classical configuration (which is defined as minimizing the classical action S), but can be in arbitrary configurations that we all have to include. The inverse cut-off then gets the physical meaning of the minimum length scale the fluctuations can assess. But this is not the only reason for us to favor the functional integral over the canonical formulation. In principle, both quantization procedures are equivalent. On the level of practical approximations, however, the functional integral approach provides us with new powerful and intuitive approximation methods. Of course, the functional integral formulation also allows for an expansion in small couplings, making it possible to recover the results of canonical perturbation theory. But aside from that, we will see that we can use the functional integral to get a much deeper understanding of the effect of fluctuations and their role in quantizing a theory. The key idea due to K. Wilson [21] is not to aim to determine the functional integral in one formal overall step, but to proceed momentum shell by momentum shell, at each step taking the effect on the Lagrangian into account.

3.1 The renormalization group idea

In order to illustrate Wilson's general idea of integrating out single momentum shells best, we first separate the functional integral from the determination of a certain Green's function. This is done by introducing a somewhat formal, but nevertheless very useful object, the generating functional Z. For the simplest case of a pure real scalar field ϕ, it is defined as

$$Z[J] = \int \mathcal{D}\phi \, e^{\, i \, S[\phi] + i \int d^d x \, J(x) \, \phi(x)},$$

where we introduced the source $J(x)$, which indeed formally acts as a source term, as can be seen when deriving the classical equations of motion. $S = \int d^d x \, \mathcal{L}$ denotes the classical action of ϕ. An arbitrary Green's function $G(x_1, ..., x_n) = \langle 0 | T \phi(x_1) ... \phi(x_n) | 0 \rangle$ can then be recovered by functional derivation according to

$$G(x_1, ..., x_n) = Z[J]^{-1} \left(-i \frac{\delta}{\delta J(x_1)} \right) \left(-i \frac{\delta}{\delta J(x_2)} \right) Z[J] \bigg|_{J \, = \, 0}.$$

Thus, the generating functional can be considered as to represent the theory in a global sense; it contains the whole theory. The generalization to more involved theories is straightforward. We mention that the generating functional has not only formally, but also conceptually many similarities to the partition function in statistical physics. In both cases, the idea behind is to perform a weighted "sum" over all states. This connection has led to a very fruitful exchange between the statistical physics and the particle physics communities.

For our further argumentation we can drop the source J, $J = 0$. We make the cut-off explicit by rewriting the path integral in momentum space:[1]

$$Z = \int [\mathcal{D}\phi]_\Lambda \, e^{- \int d^d x \, \mathcal{L}(\phi)},$$

where

$$[\mathcal{D}\phi]_\Lambda = \prod_{|k| < \Lambda} d\phi(k).$$

---

[1]From now on, we work in Euclidean space; this saves us from problems due to lightlike momenta, which can have a small absolute value $|k|$ even when the components of k are very large.

Wilson's striking idea now is to integrate just over a single momentum shell from Λ down to $b\Lambda$, with $b < 1$ very close to 1. The remaining path integral goes only up to $b\Lambda$. The generating functional Z, of course, must remain constant under this operation – we do not want to change the physics. Thus, this shell integration must be accompanied by a change of the Lagrangian, $\mathcal{L} \to \mathcal{L}_{\text{eff}}$, and our new path integral looks like

$$Z = \int [\mathcal{D}\phi]_{b\Lambda} \, e^{- \int d^d x \, \mathcal{L}_{\text{eff}}(\phi)}.$$

By iterating this procedure of integrating over infinitesimal momentum shells, we should get a smooth flow of the Lagrangian in "theory space". This is the general idea. And we can already learn a central lesson from it: that fluctuations on different scales must be treated differently, or: preceding fluctuations influence succeeding fluctuations, since the corresponding Lagrangians, which constitute the way the fluctuations influence the physics, are in general different on different scales.

In order to make quantitative progress, we have to develop explicit methods for performing this shell integration – at least approximately. Coming from canonical perturbation theory, it is most natural first to consider the case of small couplings. Here, we can formally expand the exponential in the small couplings and adopt the common language of Feynman diagrams (with classical propagators) – with the only modification that this time the loop integrations, which reflect the fluctuations in the shell, go only from $b\Lambda$ to Λ. We emphasize that this means that we do not have to bother about any kind of divergences; all integrals are finite. The resulting flow of the Lagrangian then corresponds to a flow of the interaction couplings and the propagator(s). Even though we consider just like in standard perturbation theory only contributions up to a certain order in the couplings, this backlash of fluctuations on the way succeeding fluctuations are treated results in an enormous improvement of our approximation compared to standard perturbation theory, where the same couplings and propagators are used across all scales. We get "renormalization group improved" results, in analogy to the improvement achieved when taking the running of the couplings according to the Callan-Symanzik equation into account.[2] Indeed, the Wilson β functions

---

[2] Strictly speaking, the Callan-Symanzik equation describes the change of the renormalized couplings under variations of the mass scale of the theory. We use it in a more general sense, considering variations of the renormalization scale. Originally, this was done first by Gell-Mann and Low.

and the Callan-Symanzik β functions are identical – at least at one-loop level. In the Callan-Symanzik case, the running is caused by the requirement that the Green's functions be invariant under a change of the artificial renormalization scale.[3] While standard perturbation theory only catches the "leading logarithms" of an expansion of the running coupling in the renormalized coupling, the RG improvement "resums" these logarithms to all orders, yielding just the running couplings. Therefore, the RG-improved results are valid as long as the running couplings remain small, whereas the standard perturbative results are only valid in the vicinity of the renormalization scale, when the leading logs are still small.

Can we understand this close relationship between the Wilson running couplings and the Callan-Symanzik running couplings, though they emerge from completely different formal bases? Assume we measure our couplings at a renormalization scale $\tilde{\Lambda}$. Then, roughly speaking, our measurement can only be sensitive to fluctuations above that scale; our measurement scale effectively acts as an IR cut-off. Thus, again roughly speaking, the difference of the results when measuring the couplings at two different renormalization scales $\tilde{\Lambda}_1 < \tilde{\Lambda}_2$ is due to the fluctuations in between those scales. But this is just what we do in Wilson's approach: By integrating down from $\tilde{\Lambda}_2$ to $\tilde{\Lambda}_1$, we determine the change of the couplings induced by the fluctuations in between those scales. We gain the insight that we can implement Wilson's idea of smoothly including the fluctuations by applying an arbitrary "scale-adjustable" IR cut-off, not necessarily by changing a sharp-cut-off integration limit. We will make use of this in the next section when applying a scale dependent additional mass as IR cut-off. It will be a particular advantage for the analytics to use smooth cut-off functions instead of the sharp cut-off; moreover, it avoids certain pathologies of the latter.

3.2 The exact renormalization group equation

A further important step for the usefulness of Wilson's approach was the derivation of an exact renormalization group equation for the action S by

---

[3]We are aware that we at first have to distinguish between the renormalized couplings, which are determined by measurement at the renormalization scale, and the running couplings, which are a consequence of solving the Callan-Symanzik equation. But since they both obey the same β functions, we can ignore this discrepancy.

Wegner and Houghton [22].[4] They could show that when integrating over a momentum shell of thickness t, where $b = e^t$, $b < 1$ and $1 - b$ infinitesimal (the cut-off be normalized as 1), only tree level and one-loop "Feynman" graphs[5] have to be taken into account, since they are the only ones that contribute to the flow to linear order in t. The authors still stick to the procedure of shifting a sharp cut-off integration limit. We adopt a more modern version of an exact renormalization group equation, which allows for a more general implementation of the IR cut-off [23]. It is based on the effective action Γ. In order to define the effective action properly, we first have to introduce the generating functional of connected Green's functions $W[J]$, which is determined by

$$W[J] = \ln Z[J] = \ln \int \mathcal{D}\phi \, e^{-S[\phi, J]}.$$

The effective action then is defined as the Legendre transform of $W[J]$ according to

$$\Gamma[\phi_{cl}] = -W[J] + \int d^d y \, J(y) \, \phi_{cl}(y), \tag{3.1}$$

which is a functional of the "classical" field ϕ_{cl}. ϕ_{cl} is given by the vacuum expectation value of the field operator in the presence of the source J:

$$\phi_{cl}(x) \;=\; \langle \Omega | \phi(x) | \Omega \rangle_J \;=\; \frac{\int \mathcal{D}\phi \, \phi(x) \, e^{-S[\phi, J]}}{\int \mathcal{D}\phi \, e^{-S[\phi, J]}} \;=\; \frac{\delta W}{\delta J(x)}.$$

The source J in (3.1) has to be understood as function of ϕ_{cl}. J and ϕ_{cl} can be converted by using that

$$\frac{\delta \Gamma[\phi_{cl}]}{\delta \phi_{cl}} \;=\; -\int \frac{\delta W[J]}{\delta J} \frac{\delta J}{\delta \phi_{cl}} + \int \frac{\delta J}{\delta \phi_{cl}} \phi_{cl} + J \;=\; J.$$

These definitons can be used to derive an explicit formulation of the effective action as a path integral:

$$\Gamma[\phi_{cl}] = -\ln \int \mathcal{D}\phi \, e^{-S[\phi + \phi_{cl}] + \int \frac{\delta \Gamma[\phi_{cl}]}{\delta \phi_{cl}} \phi}.$$

---

[4]Due to their statistical physics background, they related their functional integral to the partition function, thus considering the flow of the Hamiltonian H instead of the action S.

[5]We can adopt a diagrammatical language also in the general case; but this time we have to apply the full propagator.

This is a complicated functional integro-differential equation, but still we get by expansion around ϕ_{cl},

$$\Gamma[\phi_{cl}] = S[\phi_{cl}] - \ln \int \mathcal{D}\phi \, e^{-\int \left(\frac{\delta S[\phi_{cl}]}{\delta \phi} - \frac{\delta \Gamma[\phi_{cl}]}{\delta \phi_{cl}} \right) \phi - \iint \phi \frac{\delta^2 S[\phi_{cl}]}{\delta \phi \, \delta \phi} \phi - \cdots},$$

the important result that, as long as there are no fluctuations included at all, the effective action equals the classical action S.

Similar to the generating functional $Z[J]$, the effective action $\Gamma[\phi_{cl}]$ contains all information on the quantum system. This becomes manifest when realizing that the effective action can be used to recover all one-particle irreducible Green's functions.

We are looking for a differential equation that smoothly builds in the fluctuations from the cut-off Λ down to zero, thus interpolating between the classical action S and the full effective action Γ. The new idea now is that this can equally well be done by adding an additional (momentum-dependent) mass term to the original theory rather than shifting the integration limit of the path integral. This mass term acts as an IR regulator to the original theory. Changing the magnitude of this mass term thus corresponds to changing the amount of fluctuations that contribute to the effective action.[6] Effectively, of course, we define for each choice of the additional mass term a different theory, and consider for each choice the full functional integral to be determined. In other words: we shifted our objective from the determination of the flow of one and the same theory due to shell-by-shell integration of the functional integral to the determination of the "flow" that connects the fully integrated-out effective actions of the modified theories when smoothly lowering the additional mass term. Only for a vanishing additional mass term we recover the effective action of the original theory. One may argue that we apply both an IR and an UV cut-off in this approach. While we keep the UV cut-off fixed, we smoothly lower the IR cut-off. Thus, we prevent potential problems due to both UV divergencies and IR divergencies.

The action of our modified theory is defined as [7]

$$S_k[\chi] = S[\chi] + \Delta S_k[\chi],$$

---

[6]We will allow for very general choices of momentum-dependent regulators, corresponding to a vast variety of ways to damp the IR modes. Hence, it is too simplified to assume that the regulator acts as a sharp cut-off. But we think that this way the idea is illustrated best.

[7]For notational clearness, we denote in the remainder of this section the classical field by ϕ and the fluctuating quantum field by χ.

with

$$\Delta S_k[\chi] = \frac{1}{2} \int \frac{d^d q}{(2\pi)^d} \, \chi(-q) \, R_k(q) \, \chi(q).$$

We see that ΔS_k takes the formal structure of a mass term. But we allow for very general choices of the momentum dependent "mass" $R_k(q)$. Indeed, we only demand that

$$\lim_{k \to 0} R_k(q) = 0 \quad , \quad \lim_{k \to \Lambda} R_k(q) = \infty \quad \text{and} \quad \lim_{q^2/k^2 \to 0} R_k(q) > 0,$$

which guarantees that we start at $k = \Lambda$ with the classical action S and end up at $k = 0$ at the full, unregularized effective action Γ of our original theory. k denotes the scale of the onset of the damping of IR modes.

In accordance with the previous definitions, we get a modified generating functional

$$Z_k[J] = \int \mathcal{D}\chi \, e^{-S_k[\chi, J]},$$

and a modified generating functional of the connected Green's functions

$$W_k[J] = \ln Z_k[J].$$

We can interpret these modified quantities as average values of our original quantities, since the inclusion of the fluctuations from Λ to k effectively corresponds to a coarse graining process to length scales of order $1/k$. We now ask for the change of W_k under an infinitesimal change of the scale k:

$$
\begin{aligned}
\partial_t W_k &= e^{-W_k} \, \partial_t \, e^{W_k} \\
&= e^{-W_k} \int \mathcal{D}\chi \left(-\partial_t \, \Delta S_k[\chi] \right) e^{S_k[\chi, J]} \\
&= -\frac{1}{2} \int \frac{d^d q}{(2\pi)^d} \left(\partial_t R_k(q) \right) \underbrace{\frac{1}{Z_k} \int \mathcal{D}\chi \, \chi(-q) \, \chi(q) \, e^{-S_k[\chi, J]}},
\end{aligned}
$$

with $\partial_t = k \frac{\partial}{\partial k}$. So far we made only use of the definitions given above and performed the derivative with respect to t. The underbraced term corresponds to the prescription for the determination of the (average) 2-point Green's function $G_k(q) = \langle \chi(-q) \chi(q) \rangle$ (in presence of the source J). Adding a zero in terms of

$$0 = -\langle \chi(-q) \rangle \langle \chi(q) \rangle + \langle \chi(-q) \rangle \langle \chi(q) \rangle$$

20

yields

$$
\partial_t W_k = -\frac{1}{2} \int \frac{d^d q}{(2\pi)^d} \left\{ \left(\partial_t R_k(q) \right) \underbrace{\left[\langle \chi(-q)\chi(q) \rangle - \langle \chi(-q) \rangle \langle \chi(q) \rangle \right]}_{} \right.
$$
$$
\left. + \left(\partial_t R_k(q) \right) \langle \chi(-q) \rangle \langle \chi(q) \rangle \right\}.
$$

This time, the underbraced term corresponds to the (average) connected Green's function $G_{c,k}(q) = \langle \chi(-q)\chi(q) \rangle - \langle \chi(-q) \rangle \langle \chi(q) \rangle$. Applying $\phi(q) = \langle \chi(q) \rangle$ and the definition of ΔS_k, we end up with

$$
\partial_t W_k = -\frac{1}{2} \int \frac{d^d q}{(2\pi)^d} \left[\left(\partial_t R_k(q) \right) G_{c,k}(q) \right] - \partial_t \Delta S_k[\phi].
$$

Note that ΔS_k is a function of the classical field ϕ, now. Next, we switch to the flow of the effective average action $\Gamma_k[\phi]$, which is defined as

$$
\Gamma_k[\phi] = -W_k[J(\phi)] + \int d^d x \, J(x) \, \phi(x) - \Delta S_k[\phi].
$$

We get for the flow

$$
\partial_t \Gamma_k[\phi] = - \left[\partial_t W_k[J(\phi)]_{\big| J} + \int d^d x \, \frac{\delta W_k[J]}{\delta J(x)} \left(\partial_t J(x) \right) \right]
$$
$$
+ \int d^d x \left(\partial_t J(x) \right) \phi(x)
$$
$$
- \partial_t \Delta S_k[\phi]
$$
$$
= \frac{1}{2} \int \frac{d^d q}{(2\pi)^d} \left[\left(\partial_t R_k(q) \right) G_{c,k}(q) \right],
$$

since $\frac{\delta W_k[J]}{\delta J(x)} = \phi(x)$. Last, we formulate the Greens function as functional derivative of the effective average action:

$$
G_k = \frac{\delta^2 W}{\delta J \, \delta J} = \frac{\delta \phi}{\delta J} = \left(\frac{\delta J}{\delta \phi} \right)^{-1} = \left(\frac{\delta^2 \Gamma_k}{\delta \phi \, \delta \phi} + R_k \right)^{-1}.
$$

Thus, our final result reads

$$
\partial_t \Gamma_k = \frac{1}{2} \int \frac{d^d q}{(2\pi)^d} \left(\partial_t R_k(q) \right) \left(\frac{\delta \Gamma_k}{\delta \phi(-q) \, \delta \phi(q)} + R_k(q) \right)^{-1}.
$$

21

$$\partial_t \Gamma_k = \frac{1}{2} \quad$$

Figure 3.1: Diagrammatical interpretation of the exact renormalization group flow equation (3.2).

This is a functional differential equation. For more involved theories, for example including fermions or fields with inner indices, we can formulate it in a slightly symbolic, basis-independent form [23]:

$$\partial_t \, \Gamma_k = \frac{1}{2} \, \mathrm{STr} \left\{ \left(\Gamma_k^{(2)} + R_k \right)^{-1} \left(\partial_t \, R_k \right) \right\}. \tag{3.2}$$

The "super"trace is taken over all spaces, inner and outer, where the "super" stands for the obligatory minus sign accompanying fermionic sectors. Equation (3.2) can be depicted by a one-loop diagram, as shown in Figure 3.1. The double line denotes the full (average) propagator $\left(\Gamma_k^{(2)} + R_k \right)^{-1}$. $\Gamma_k^{(2)}$ is called the (k-dependent) fluctuation matrix. The dot symbolizes the factor $\left(\partial_t R_k \right)$, which acts as a "weighting factor" to the fluctuations.

Approximating the ERGE Equation (3.2) will be the starting point for the derivations of all of our flow equations. If we think of the effective average action in a derivative expansion $(\rho = \frac{1}{2}\phi^2)$,[8]

$$
\begin{aligned}
\Gamma_k[\phi] \;\; = \;\; & \int d^d x \Big\{ U_k(\rho) \\
& + \frac{1}{2} \, Z_k^0 \, \partial_\mu \phi \, \partial^\mu \phi + Z_k^1 \, \rho \, \partial_\mu \phi \, \partial^\mu \phi + ... \\
& + \frac{1}{4} \, Y_k^0 \, \partial_\mu \rho \, \partial^\mu \rho + Y_k^1 \, \rho \, \partial_\mu \rho \, \partial^\mu \rho + ... \\
& + \mathcal{O}(\partial^4) \Big\},
\end{aligned}
$$

we see that (3.2) describes a set of infinitely many coupled differential equations. We do not have tools to solve such a vast system exactly. Hence, we

---

[8]We allow only for operators that are invariant under a given symmetry. In our case, this symmetry is parity.

22

have to develop methods to approximate. The most straightforward way is just to take this expansion and truncate it, restricting oneselve to a manage-able subset of expansion terms. This corresponds to considering a projected flow, where we project onto the hyper plane in theory space spanned by our truncation. However, the projected trajectory is not the projection of the exact trajectory in "theory space", since we do not take the influence of the neglected operators into account. We emphasize that the particular choice of our truncation completely determines the structure of the fluctuation matrix $\Gamma_k^{(2)}$ on the RHS of (3.2); in other words: The RHS only depends on the ex-pansion coefficients of the operators that we include in our truncation. Thus, the set of flow equations for these coefficients is closed. We determine the flow equation of a particular coefficient by applying the corresponding pro-jection rule on (3.2). A projection rule imposes conditions on the fields that effectively isolates the designated operator. We will give explicit examples in the next chapter, when we derive the flow equations for the coefficients of our Toy Model truncation. Of course, we could also project onto an operator $\widehat{\mathcal{O}}$ that is not included in our truncation. We only have to be aware that the resulting flow is merely a consequence of the operators in our truncation; the flow of $\widehat{\mathcal{O}}$ itself has no backlash on the way succeeding fluctuations are integrated out.

Chapter 4

Renormalization group analysis of our Toy Model

So far, we have boiled the Standard Model down to a Toy Model convenient for our issue, which consists merely of one self-interacting real scalar field σ and one non-self-interacting fermionic field ψ, representing the Higgs particle and the top quark respectively. The two fields are coupled via a Yukawa interaction. We have defined the corresponding quantum field theory in a functional integral formulation. In the last chapter we introduced a sophisticated method of how to evaluate such functional integrals, namely by exact renormalization group equations. Now we want to apply this method to our Toy Model.

4.1 Truncating our Toy Model

We want to determine the RG flow of the effective average action $\Gamma_k[\sigma, \psi, \overline{\psi}]$ of our Toy Model[1]. But as mentioned before, we cannot solve (3.2) exactly. Given we start with a non-trivial cut-off action, we have to expect all kinds of operators to be generated in the course of the flow, resulting in an arbitrarily complex structure.[2] It is obvious that we cannot keep track of all these operators. We have to restrict ourselves to a manageable amount of operators

---

[1] We denote both the original quantum fields and the classical fields in terms of which the effective action is formulated with σ and ψ, respectively.

[2] More precisely, we expect all operators to be generated that are not excluded by symmetry.

that we take into account for the effective action or rather the fluctuation matrix on the RHS. We emphasize that this does not necessarily mean that we have to restrict ourselves to a finite number of operators – at least not on the level of deriving the flow equations. Actually, we will soon motivate that even our truncation[3] should contain infinitely many operators.

So how do we establish a reasonable truncation for our Toy Model? Ideally, we would demand that the truncated RG trajectory in "theory space" should be close to the exact one, or in other words: The exact RG trajectory should run as close as possible to the hyper plane that we are projecting on. Unfortunately there is no a priori way of determining a good truncation. This is closely connected to the fact that there does not exist a way of estimating the absolute error caused by a certain truncation.[4] Aside from that, in general the exact trajectory strongly depends on the "starting point" in theory space, the cut-off action. Therefore, we have to follow another, more pragmatic and robust approach. We will construct our truncation from "bottom up": We start with the minimum collection of operators our truncation must embrace in order to be able to reproduce the defining physical properties of our Toy Model. Those properties are roughly: both bosonic and fermionic fluctuations drive the flow of the scalar effective average potential, the first due to its self interaction, the latter via the Yukawa interaction, which eventually results in the emergence of a vacuum expectation value (if there is not already one right from the start), which in turn gives the fermion its mass. The final shape of the scalar potential then also sets the mass of the Higgs particle. So which ingredients do we need for this purpose? In order to be able to flucutuate at all, we first have to make the fields dynamical by providing propagators; the simplest realizations of them are via the classical kinetic terms $\frac{1}{2} \left(\partial_\mu \sigma(x) \right) \left(\partial^\mu \sigma(x) \right)$ and $\overline{\psi}(x) \, i\partial\!\!\!/ \, \psi(x)$. The boson may have an arbitrary mass term $m^2 \sigma(x)^2$, whereas the fermion acquires a mass solely via the Yukawa interaction, when there is a vacuum expectation value. Then we need, of course, a bosonic self-interaction and a Yukawa interaction: here the simplest choices are $\tilde{\lambda} \, \sigma(x)^{2n}$ with $n > 1$ [5] and $i\overline{h} \, \sigma(x) \, \overline{\psi}(x) \, \psi(x)$. Thus, the

---

[3]"Truncation" is the technical term for an approximation to the effective action for instance by neglecting operators in a derivative expansion. We use it in the more general sense of a "functional that constitutes the structure of the fluctuation matrix $\Gamma_k^{(2)}$".

[4]Whereas relative error estimates can be gained by comparing different truncations.

[5]Due to the required symmetry of the model, we allow only even powers of σ. We emphasize that we do not have to exclude operators with negative mass dimensions!

simplest possible truncation of our Toy Model reads

$$\Gamma \;=\; \int d^d x \Big[\frac{1}{2} \left(\partial_\mu \sigma(x) \right) \left(\partial^\mu \sigma(x) \right) + m^2 \sigma(x)^2 + \tilde{\lambda}\, \sigma(x)^{2n}$$

$$+ \overline{\psi}(x)\, i \slashed{\partial}\, \psi(x) + i\overline{h}\, \sigma(x)\, \overline{\psi}(x)\, \psi(x) \Big]. \tag{4.1}$$

Whether a vacuum expectation value is generated or not depends on the particular choice of the parameters m, $\tilde{\lambda}$ and $\overline{h}$. Note that so far the truncation is not k dependent; this does not mean that our effective average action is independent of k, but just that fluctuations on all scales are treated in the same way. Actually, this is just what is done in straightforward perturbation theory. Nevertheless, it is clear that (4.1) is too rough for our issue. After all, the decoupling of the fluctuation matrix from the actual structure of the effective average action at a certain scale k is just an artefact of our truncation. Taking (3.2) literally, the fluctuation matrix is completely determined by the structure of Γ_k at a certain scale. The fluctuations should have at least some back-effect on the way further fluctuations are integrated out. Thus, it is only fair to take at least the flow of the operators that constitute (4.1) into account. By this means, the improved truncation reads

$$\Gamma_k \;=\; \int d^d x \Big[\frac{Z_{\sigma,k}}{2} \left(\partial_\mu \sigma(x) \right) \left(\partial^\mu \sigma(x) \right) + m_k^2\, \sigma(x)^2 + \tilde{\lambda}_k\, \sigma(x)^{2n}$$

$$+ Z_{\psi,k}\, \overline{\psi}(x)\, i \slashed{\partial}\, \psi(x) + i\overline{h}_k\, \sigma(x)\, \overline{\psi}(x)\, \psi(x) \Big].$$

In a last step, we want to get rid of the artificial choice of the scalar self-interaction. Since all operators of the form σ^{2n} can be generated or even be there right from the start, it is not justifiable to favor one or finitely many of them. We have to admit all of them. Our final truncation is therefore given by

$$\Gamma_k \;=\; \int d^d x \Big[U_k\big(\sigma(x)\big) + \frac{Z_{\sigma,k}}{2} \left(\partial_\mu \sigma(x) \right) \left(\partial^\mu \sigma(x) \right)$$

$$+ Z_{\psi,k}\, \overline{\psi}(x)\, i \slashed{\partial}\, \psi(x) + i\, \overline{h}_k\, \sigma(x) \overline{\psi}(x) \psi(x) \Big]. \tag{4.2}$$

We emphasize that σ denotes the deviation from the vacuum, which only in the symmetric regime coincides with a vanishing scalar field. In general, the

26

minimum of the potential can be at any value of the field; in that case we want our truncation to display the dynamics of the field fluctuations relative to this vacuum, which, of course, corresponds to the definition of the Higgs particle. From this point of view, we rather should formulate our truncation in terms of $\Delta\sigma(x)$, where $\sigma(x) = \sigma_{\mathrm{vev}} + \Delta\sigma(x)$, with σ_{vev} being the vacuum expectation value of the scalar.

Some more remarks on the choice of our truncation: We are aware that we have founded our truncation rather on arguments of necessity and naturalness than on the proximity to the exact trajectory. We on purpose avoided to argue in terms of any kind of expansion, since we just do not have any idea of how to establish a quantitative approximation to the exact flow in the non-perturbative regime. So, even though our truncation takes the form of a derivative expansion, this does not mean that we have control over the error made by our truncation in the sense that the neglected operators yield only small corrections.[6] Aside from that, an ansatz in terms of a derivative expansion is, of course, most useful with respect to a systematic estimate of the relative error, which is achieved by comparing the original truncation with extended versions. This reasoning follows the logic that it can be considered a hint for the validity of a truncation when the coefficients of later added operators remain small in the course of the flow. Such an investigation indeed was done for our truncation in a different physical context [24]; there it proved to be reasonable. In contrast to other approaches like perturbation theory, we are at least able to investigate the non-perturbative regime, at all. And after all, our truncation is definitely a good approximation in the small-coupling regime. Last, we mention that we can consider the anomalous dimensions as very rough indicators for the quality of the approximations to the true propagators. This will be the case when the anomalous dimensions are small.

Since it proves to be convenient to derive the flow equations in momentum space, we formulate our truncation in momentum space. Applying the

---

[6]Actually, the same accounts to perturbation theory: Due to the ill-definedness of the expansion in the couplings, we cannot a priori be sure that the first neglected order only yields a small correction.

following conventions for the Fourier transformations:

$$\sigma(x) \;=\; \int \frac{d^d q}{(2\pi)^d}\, \sigma(q)\, e^{iqx},$$

$$\psi(x) \;=\; \int \frac{d^d q}{(2\pi)^d}\, \psi(q)\, e^{iqx},$$

$$\overline{\psi}(x) \;=\; \int \frac{d^d q}{(2\pi)^d}\, \overline{\psi}(q)\, e^{-iqx},$$

we get

$$\Gamma_k \;=\; \int d^d x\, U_k\big(\sigma(x)\big) + \int \frac{d^d q}{(2\pi)^d}\left[\frac{Z_{\sigma,k}}{2}\, \sigma(q)\, q^2\, \sigma(-q)\right.$$

$$\left. -Z_{\psi,k}\,\overline{\psi}(q)\slashed{q}\;\psi(q) + \int \frac{d^d p}{(2\pi)^d}\, i\,\overline{h}_k\, \sigma(p-q)\,\overline{\psi}(p)\,\psi(q)\right]. \quad (4.3)$$

The fluctuation matrix   The task will now be to derive the flow equations for the k-dependent quantities in our truncation. For this purpose, we have to determine the fluctuation matrix $\left(\Gamma_k^{(2)}(p,q)\right)_{ab}$ (a and b denote the scalar field and the spinor components of the fermion field) following from our truncation (4.3). It constitutes the way we integrate out fluctuations. The fluctuation matrix is defined by

$$\Gamma_k^{(2)}(p,q) \;:=\; \begin{pmatrix} \frac{\overrightarrow{\delta}}{\delta\sigma(-p)} \\[4pt] \frac{\overrightarrow{\delta}}{\delta\psi^T(-p)} \\[4pt] \frac{\overrightarrow{\delta}}{\delta\overline{\psi}(p)} \end{pmatrix} \Gamma_k \left(\frac{\overleftarrow{\delta}}{\delta\sigma(q)} \quad,\quad \frac{\overleftarrow{\delta}}{\delta\psi(q)} \quad,\quad \frac{\overleftarrow{\delta}}{\delta\overline{\psi}^T(-q)} \right)$$

$$=\; \begin{pmatrix} \frac{\overrightarrow{\delta}}{\delta\sigma(-p)}\Gamma_k\frac{\overleftarrow{\delta}}{\delta\sigma(q)} & \frac{\overrightarrow{\delta}}{\delta\sigma(-p)}\Gamma_k\frac{\overleftarrow{\delta}}{\delta\psi(q)} & \frac{\overrightarrow{\delta}}{\delta\sigma(-p)}\Gamma_k\frac{\overleftarrow{\delta}}{\delta\overline{\psi}^T(-q)} \\[8pt] \frac{\overrightarrow{\delta}}{\delta\psi^T(-p)}\Gamma_k\frac{\overleftarrow{\delta}}{\delta\sigma(q)} & \frac{\overrightarrow{\delta}}{\delta\psi^T(-p)}\Gamma_k\frac{\overleftarrow{\delta}}{\delta\psi(q)} & \frac{\overrightarrow{\delta}}{\delta\psi^T(-p)}\Gamma_k\frac{\overleftarrow{\delta}}{\delta\overline{\psi}^T(-q)} \\[8pt] \frac{\overrightarrow{\delta}}{\delta\overline{\psi}(p)}\Gamma_k\frac{\overleftarrow{\delta}}{\delta\sigma(q)} & \frac{\overrightarrow{\delta}}{\delta\overline{\psi}(p)}\Gamma_k\frac{\overleftarrow{\delta}}{\delta\psi(q)} & \frac{\overrightarrow{\delta}}{\delta\overline{\psi}(p)}\Gamma_k\frac{\overleftarrow{\delta}}{\delta\overline{\psi}^T(-q)} \end{pmatrix}.$$

Performing the functional derivatives yields

$$\Gamma_k^{(2)}(p,q) =$$

$$
= \left(
\begin{array}{c|c|c}
\begin{array}{c} Z_{\sigma,k}\, p^2\, \delta_{p,q} \\[2pt] +\int d^d x\, U_k''(\sigma(x))\, e^{i(q-p)x} \end{array} & i\overline{h}_k \overline{\psi}(q-p) & -i\,\overline{h}_k\, \psi^T(p-q) \\[6pt]
\hline
-i\,\overline{h}_k\, \overline{\psi}^T(q-p) & 0 & \begin{array}{c} -Z_{\psi,k}\, p\!\!\!/^{\,T}\delta_{q,p} \\[2pt] -i\,\overline{h}_k\, \sigma(p-q) \end{array} \\[6pt]
\hline
i\,\overline{h}_k\, \psi(p-q) & \begin{array}{c} -Z_{\psi,k}\, p\!\!\!/\, \delta_{p,q} \\[2pt] +i\,\overline{h}_k\, \sigma(p-q) \end{array} & 0
\end{array}
\right), \qquad (4.4)
$$

where primes denote derivatives with respect to σ.

The regulator In order to evaluate the ERGE (3.2), we still need to know one more ingredient, namely the regulator matrix $R_k(p,q)$, which acts as an IR cut-off on the fluctuations. It takes care of the shell-by-shell integration of the fluctuations, therefore making a smooth RG flow possible. We determine its general structure by remembering that we can implement an IR cut-off by imposing additional, artificial, k-dependent masses on the fields. Therefore, the matrix elements affected by the regulator should be those, which are in charge of the masses of the fields. For the scalar field, this is the σ^2 operator, for the fermion field the $\overline{\psi}\psi$ and the $\psi^T\overline{\psi}^T$ operators. We demand that the regulator nestles to the propagators according to a common mass term. Thus, the structure of the regulator is given by

$$
R_k(p,q) = \begin{pmatrix} R_{kB}(q) & 0 & 0 \\ 0 & 0 & -R_{kF}^T(-q) \\ 0 & R_{kF}(q) & 0 \end{pmatrix} \delta_{p,q}.
$$

Since we will formulate the flow equations in renormalized, dimensionless quantities, it is convenient to write

$$
R_k(p,q) = \begin{pmatrix} Z_{\sigma,k}\, q^2\, r_{kB}(q) & 0 & 0 \\ 0 & 0 & -Z_{\psi,k}\, q\!\!\!/^{\,T} r_{kF}(-q) \\ 0 & -Z_{\psi,k}\, q\!\!\!/\, r_{kF}(q) & 0 \end{pmatrix} \delta_{p,q}, \quad (4.5)
$$

where r_{kB} and r_{kF} are the dimensionless cut-off functions. This form makes explicit that we do not break rescaling invariance. $r_k(q) = r(q^2/k^2)$ guarantees that k equals the IR cut-off scale. We do not specify r_{kB} and r_{kF}

any further for the derivation of our flow equations, because a truncated flow results in an unphysical dependence of the integrated-out quantities on the particular choice of the cut-off functions. We therefore should make it our objective to implement the flow for various choices of the cut-off functions, to get an estimate of the error made by the choice of our regulator. A convenient selection is given by the linear cut-off and the sharp cut-off functions, which in some sense constitute the "best" and the "worst" choice [25].

4.2   Flow equation for the scalar potential

We begin with the derivation of the flow equation for the scalar potential $U_k(\sigma)$. As mentioned in the previous chapter, we have to apply the corresponding projection rule on the ERGE (3.2). If we think of the effective action as a derivative expansion, it is easy to see that we can isolate the scalar potential by demanding that the scalar field $\sigma(x)$ be constant, $\sigma(x) = \sigma_0 = \text{const}$, and that the fermion field vanishes: $\psi(x) = \overline{\psi}(x) = 0$. Therefore, the flow equation for the scalar potential results from the following prescription:

$$
\partial_t U_k = \frac{1}{2} \text{STr} \left[\left(\partial_t R_k(p,q) \right) \left(\Gamma_k^{(2)}(p,q) + R_k(p,q) \right)^{-1} \right] \Bigg|_{\substack{\sigma = \sigma_0 \\ \psi = \overline{\psi} = 0}} . \quad (4.6)
$$

We can safely interchange the trace and the projection rules, which renders the fluctuation matrix (4.4) diagonal in momentum space. As the regulator (4.5) is diagonal in momentum space right from the start, we can directly

30

invert $\left(\Gamma_k^{(2)}(p,q) + R_k(p,q)\right)$, yielding

$$\left(\Gamma_k^{(2)}(p,q) + R_k(p,q)\right)^{-1} =$$

$$= \delta_{p,q} \begin{pmatrix} \dfrac{1}{Z_{\sigma,k}\,P(p)+U_k''(\sigma_0)} & 0 & 0 \\[2ex] \hline 0 & 0 & \dfrac{-Z_{\psi,k}\left(1+r_{k,F}(p)\right)}{Z_{\psi,k}^2\,P_F(p)+\overline{h}_k^2\sigma_0^2}\,\slashed{p} \\ & & -\dfrac{i\overline{h}_k\,\sigma_0}{Z_{\psi,k}^2\,P_F(p)+\overline{h}_k^2\,\sigma_0^2} \\[2ex] \hline 0 & \dfrac{-Z_{\psi,k}\left(1+r_{k,F}(p)\right)}{Z_{\psi,k}^2\,P_F(p)+\overline{h}_k^2\sigma_0^2}\,\slashed{p}^T & 0 \\ & +\dfrac{i\overline{h}_k\,\sigma_0}{Z_{\psi,k}^2\,P_F(p)+\overline{h}_k^2\,\sigma_0^2} & \end{pmatrix}, \qquad (4.7)$$

where we have introduced the (massless) inverse average proapagators $P(q) = q^2\left(1+r_{k,B}(q)\right)$ and $P_F(q) = q^2\left(1+r_{k,F}(q)\right)^2$, and have used that $r_{k,F}(p) = r_{k,F}(-p)$. Multiplication of (4.7) with $\left(\partial_t R_k(p,q)\right)$ yields an operator, which is diagonal in all its indices exept for the spinor indices. We perform the trace over the inner indices, taking into account that the "Supertrace" causes a minus sign in the fermionic sector and using standard identities to resolve the Dirac traces. We get

$$\partial_t U_k = \frac{1}{2}\,Z_{\sigma,k}\int\frac{d^dp}{(2\pi)^d}\frac{\left(\partial_t R_{k,B}(p)\right)}{P(p)+Z_{\sigma,k}^{-1}U_k''}$$

$$-d_\gamma\,Z_{\psi,k}\int\frac{d^dp}{(2\pi)^d}\frac{\left(1+r_{k,F}(p)\right)p^2\left[\partial_t\left(Z_{\psi,k}\,r_{k,F}(p)\right)\right]}{P_F(p)+Z_{\psi,k}^{-2}\,\overline{h}_k^2\,\sigma_0^2}, \quad (4.8)$$

where d_γ denotes the dimension of the Gamma matrices. We can write equation (4.8) in a more compact way by introducing the dimensionless threshold functions $l_0^d(\omega;\eta_\sigma)$ and $l_0^{(F)\,d}(\omega;\eta_\psi)$, which contain all momentum integrations. The definitions of the threshold functions can be looked up in Appendix A. The anomalous dimensions are defined as $\eta_\sigma = -\partial_t\ln Z_{\sigma,k}$ and

31

$\eta_\psi = -\partial_t \ln Z_{\psi,k}$. We end up with

$$\begin{aligned}
\partial_t U_k &= 2\, v_d\, k^d \left[l_0^d \left(k^{-2}\, Z_{\sigma,k}^{-1}\, \left[2\,\rho\, U_k'' + U_k' \right]; \eta_\sigma \right) \right. \\
&\qquad \left. - d_\gamma\, l_0^{(F)\,d} \left(2\, k^{-2}\, Z_{\psi,k}^{-2}\, \overline{h}_k^2\, \rho; \eta_\psi \right) \right],
\end{aligned} \qquad (4.9)$$

where the primes denote derivatives with respect to the field invariant $\rho = \frac{1}{2}\sigma_0^2$, and $v_d^{-1} = 2^{d+1}\, \pi^{d/2}\, \Gamma(d/2)$. In order to be able to implement this equation numerically, we have to make it dimensionless: all quantities must be represented by pure numbers. This is performed by dividing all dimensionful quantities by some appropriate power of the same dimensionful quantity, for example a typical scale of the theory. We employ two different options:

Dimensionless form by fixed-scale division   The most obvious way to make quantities dimensionless is just by dividing them by a fixed scale, for example the cut-off Λ. We will employ this method at the onset of the "freeze-out" of the flow, therefore naturally dividing by this freeze-out scale. For more information on this topic we refer to Section 5.3. Here, we derive the corresponding equation for some arbitrary fixed scale $\overline{\Lambda}$. We use the redefinition in dimensionless quantities to simultaneously renormalize them. We define the renormalized, dimensionless field strength

$$\check{\rho} = Z_\sigma\, \overline{\Lambda}^{\,2-d}\, \rho,$$

the renormalized, dimensionless Yukawa coupling

$$\check{h}_k^2 = Z_\sigma^{-1}\, Z_\psi^{-2}\, \overline{\Lambda}^{\,d-4}\, \overline{h}_k^2,$$

and the dimensionless potential

$$\check{u}_k = U_k\, \overline{\Lambda}^{\,-d}.$$

Then we get

$$\begin{aligned}
\partial_t \check{u}_k &= \check{u}_k'\, \check{\rho}\, \eta_\sigma \\
&\quad + 2\, v_d\, \left(k/\overline{\Lambda} \right)^d \left[l_0^d \left((k/\overline{\Lambda})^{-2}\, [2\,\check{\rho}\, \check{u}_k'' + \check{u}_k'], \eta_\sigma \right) \right. \\
&\qquad \left. - d_\gamma\, l_0^{(F)\,d} \left((k/\overline{\Lambda})^{-2}\, 2\, \check{\rho}\, \check{h}_k^2, \eta_\psi \right) \right],
\end{aligned} \qquad (4.10)$$

where the term in the first line is due to the renormalization of the field strength. Here, primes denote derivatives with respect to $\check{\rho}$.

Dimensionless form by running-scale division Another possibility to define dimensionless quantities is given by the regulator scale k, that we are naturally provided with. This time, we define the renormalized, dimensionless field strength according to

$$\tilde{\rho} = Z_\sigma \, k^{2-d} \rho,$$

the renormalized, dimensionless Yukawa coupling according to

$$h_k^2 = Z_\sigma^{-1} \, Z_\psi^{-2} \, k^{d-4} \, \overline{h}_k^2,$$

and the dimensionless potential by

$$u_k = U_k \, k^{-d}.$$

Now, we get

$$
\begin{aligned}
\partial_t u_k \;=\; & -d \, u_k + (d - 2 + \eta_\sigma) \, \tilde{\rho} \, u_k' \\
& + 2 \, v_d \left[l_0^d \left(u_k' + 2 \, \tilde{\rho} \, u_k'', \eta_\sigma \right) \right. \\
& \hspace{2em} \left. - d_\gamma \, l_0^{(F)\,d} \left(2 \, \tilde{\rho} \, h_k^2, \eta_\psi \right) \right],
\end{aligned}
\tag{4.11}
$$

where the term in the first line has additional contributions due to the running of k. This time, of course, primes denote derivatives with respect to $\tilde{\rho}$. By convention, we will refer to equation (4.11) in the sequel just as 'dimensionless' potential flow equation.

4.3   Flow equation for the Yukawa coupling

Second, we derive the flow equation for the (squared)[7] Yukawa coupling h_k^2. In order to find the corresponding projection rule, we have to take into account that only the deviation from the vacuum expectation value $\Delta\sigma(x)$ dynamically results in an interaction with the fermion field, whereas the vacuum expectation value σ_{vev} itself acts as a mass term to the fermions. Thus, the Yukawa coupling is attained by projecting onto the operator $\Delta\sigma\overline{\psi}\psi$ rather

---

[7]It is a certain feature of the symmetry of our system that the Yukawa coupling appears only in powers of its square.

than by projecting onto $\sigma \overline{\psi} \psi$. The projection rule for the Yukawa coupling therefore reads

$$\overline{h}_k = \frac{1}{i} \frac{\delta}{\delta \Delta \sigma(p')} \frac{\overrightarrow{\delta}}{\delta \overline{\psi}(p)} \Gamma_k \frac{\overleftarrow{\delta}}{\delta \psi(q)} \bigg|_{\substack{\psi = \overline{\psi} = \Delta \sigma = 0 \\ p' = p = q = 0}} .$$

Using (3.2), the corresponding flow equation follows from

$$\partial_t \overline{h}_k =$$

$$= \frac{1}{2i} \frac{\delta}{\delta \Delta \sigma(p')} \frac{\overrightarrow{\delta}}{\delta \overline{\psi}(p)} \mathrm{STr} \left[\left(\partial_t R_k \right) \left(\Gamma_k^{(2)} + R_k \right)^{-1} \right] \frac{\overleftarrow{\delta}}{\delta \psi(q)} \bigg|_{\substack{\Delta \sigma = 0 \\ \psi = \overline{\psi} = 0 \\ p' = p = q = 0}}$$

$$= \frac{1}{2i} \frac{\delta}{\delta \Delta \sigma(p')} \frac{\overrightarrow{\delta}}{\delta \overline{\psi}(p)} \mathrm{STr} \left[\tilde{\partial}_t \ln \left(\Gamma_k^{(2)} + R_k \right) \right] \frac{\overleftarrow{\delta}}{\delta \psi(q)} \bigg|_{\substack{\psi = \overline{\psi} = \Delta \sigma = 0 \\ p' = p = q = 0}} .$$

In the last line we have introduced the operator $\tilde{\partial}_t$, which is defined to act only on the t dependence of the regulator R_k. It is convenient to delay the t derivative until the very end of the calculation, when all the other algebra is done, because it blows up the number of terms.

This time we are not free to apply the vanishing of the fields, $\Delta \sigma = \psi = \overline{\psi} = 0$, before taking the functional derivatives. Thus, we have to deal with a fluctuation matrix that is not diagonal in its momentum indices. If we think of the operator within the Supertrace in an expansion in the fields $\Delta \sigma$, ψ and $\overline{\psi}$, the projection rule tells us that only those expansion terms "survive" the projection, which both contain each field exactly once and do not contain a derivative of any field at all. So, we only have to regard the terms, which fulfill these restrictions. To make them manifest, we want to expand the operator $\ln \left(\Gamma_k^{(2)} + R_k \right)$ in powers of the fields $\Delta \sigma$, ψ and $\overline{\psi}$, keeping only those terms, which at least provide a chance to fulfill the restrictions. For this purpose, we isolate the fields by decomposing the operator $\left(\Gamma_k^{(2)} + R_k \right)$ into a propagator part and a field part:

$$\left(\Gamma_k^{(2)} + R_k \right) = \left(\Gamma_{k,0}^{(2)} + R_k \right) + \Delta \Gamma_k^{(2)}, \tag{4.12}$$

where $\left(\Gamma_{k,0}^{(2)} + R_k\right)$ contains all components independent of the fluctuating fields $\Delta\sigma, \psi, \overline{\psi}$, whereas $\Delta\Gamma_k^{(2)}$ contains exclusively the field-dependent components. By inspection of (4.4) and (4.5), and by applying $\sigma(p) = \sigma_{\text{vev},k}\,\delta_{0,p} + \Delta\sigma(p)$, we find

$$\left(\Gamma_{k,0}^{(2)} + R_k\right) =$$

$$= \delta_{p,q} \begin{pmatrix} Z_{\sigma,k}\,p^2\left(1+r_{k,B}(p)\right) & 0 & 0 \\ +U_k''(\sigma_{\text{vev},k}) & & \\ & & \\ 0 & 0 & -Z_{\psi,k}\,\slashed{p}^T\left(1+r_{k,F}(-p)\right) \\ & & -i\,\overline{h}_k\,\sigma_{\text{vev},k} \\ & & \\ 0 & -Z_{\psi,k}\,\slashed{p}\left(1+r_{k,F}(p)\right) & 0 \\ & +i\,\overline{h}_k\,\sigma_{\text{vev},k} & \end{pmatrix} \tag{4.13}$$

and

$$\Delta\Gamma_k^{(2)} = \begin{pmatrix} U_k'''(\sigma_{\text{vev},k})\,\Delta\sigma(p-q) & i\,\overline{h}_k\,\overline{\psi}(q-p) & -i\,\overline{h}_k\,\psi^T(p-q) \\ & & \\ -i\,\overline{h}_k\,\overline{\psi}^T(q-p) & 0 & -i\,\overline{h}_k\,\Delta\sigma(p-q) \\ & & \\ i\,\overline{h}_k\,\psi(p-q) & i\overline{h}_k\,\Delta\sigma(p-q) & 0 \end{pmatrix}. \tag{4.14}$$

We have already used here that we can neglect all terms beyond first order in the expansion

$$\int d^d x\, U_k''\big(\sigma_{\text{vev},k} + \Delta\sigma(x)\big)\, e^{i\,(q-p)\,x}$$

$$= \int d^d x\left[U_k''(\sigma_{\text{vev},k}) + U_k'''(\sigma_{\text{vev},k})\,\Delta\sigma(x) + ...\right] e^{i\,(q-p)\,x} \tag{4.15}$$

$$= U_k''(\sigma_{\text{vev},k})\,\delta_{q,p} + U_k'''(\sigma_{\text{vev},k})\,\Delta\sigma(p-q) + ...,$$

as higher powers of $\Delta\sigma$ would not survive the projection.

The propagator part (4.13) is diagonal in its momentum indices and therefore can be inverted, which will be crucial for the expansion of the logarithm. Actually, it is just the fluctuation matrix (4.4) with $\sigma(x) = \sigma_{\text{vev}}$ and $\psi = \overline{\psi} = 0$, in analogy to the projected fluctuation matrix in the derivation of the

flow equation for the scalar potential. Thus, we get the same inverse, except for the replacement $\sigma_0 \to \sigma_{\mathrm{vev},k}$:

$$\left(\Gamma_{k,0}^{(2)} + R_k\right)^{-1} = \delta_{p,q} \times$$

$$\begin{pmatrix} \dfrac{1}{Z_{\sigma,k}\,P(p)+U_k''(\sigma_{\mathrm{vev},k})} & 0 & 0 \\[2em] 0 & 0 & \begin{aligned}&\dfrac{-Z_{\psi,k}\left(1+r_{k,F}(p)\right)}{Z_{\psi,k}^2\,P_F(p)+\overline{h}_k^2\sigma_{\mathrm{vev},k}^2}\,\slashed{p}\\ &-\dfrac{i\overline{h}_k\,\sigma_{\mathrm{vev},k}}{Z_{\psi,k}^2\,P_F(p)+\overline{h}_k^2\,\sigma_{\mathrm{vev},k}^2}\end{aligned} \\[3em] 0 & \begin{aligned}&\dfrac{-Z_{\psi,k}\left(1+r_{k,F}(p)\right)}{Z_{\psi,k}^2\,P_F(p)+\overline{h}_k^2\sigma_{\mathrm{vev},k}^2}\,\slashed{p}^T\\ &+\dfrac{i\overline{h}_k\,\sigma_{\mathrm{vev},k}}{Z_{\psi,k}^2\,P_F(p)+\overline{h}_k^2\,\sigma_{\mathrm{vev},k}^2}\end{aligned} & 0 \end{pmatrix} \quad (4.16)$$

We bring the operator $\ln\left(\Gamma_k^{(2)} + R_k\right)$ into a form suitable for expansion by writing

$$\mathrm{STr}\left[\tilde{\partial}_t \ln\left(\Gamma_k^{(2)} + R_k\right)\right] = \mathrm{STr}\left[\tilde{\partial}_t \ln\left(\Gamma_{k,0}^{(2)} + \Delta\Gamma_k^{(2)} + R_k\right)\right]$$

$$= \mathrm{STr}\left[\tilde{\partial}_t \ln\left\{\left(\Gamma_{k,0}^{(2)} + R_k\right)\left(1 + \left(\Gamma_{k,0}^{(2)} + R_k\right)^{-1}\Delta\Gamma_k^{(2)}\right)\right\}\right]$$

$$= \mathrm{STr}\left[\tilde{\partial}_t \ln\left(\Gamma_{k,0}^{(2)} + R_k\right)\right] + \mathrm{STr}\left[\tilde{\partial}_t \ln\left\{\left(1 + \left(\Gamma_{k,0}^{(2)} + R_k\right)^{-1}\Delta\Gamma_k^{(2)}\right)\right\}\right].$$

Next, we apply the Taylor expansion of the logarithm: $\ln(1+x) = x - \frac{1}{2}x^2 + \frac{1}{3}x^3 + \dots$. It is crucial to realize that only the term cubic in $\Delta\Gamma_k^{(2)}$ survives the projection, as it is the only one that contains each field exactly once. Thus, the projection rule for the flow equation simplifies to

$$\partial_t \overline{h}_k =$$

$$= \frac{1}{6i}\frac{\delta}{\delta\Delta\sigma(p')}\frac{\overrightarrow{\delta}}{\delta\overline{\psi}(p)}\,\mathrm{STr}\left[\tilde{\partial}_t\left\{\left(\Gamma_{k,0}^{(2)} + R_k\right)^{-1}\Delta\Gamma_k^{(2)}\right\}^3\right]\frac{\overleftarrow{\delta}}{\delta\psi(q)}\Bigg|_{\substack{\psi=\overline{\psi}=\Delta\sigma=0\\ p'=p=q=0}}.$$

36
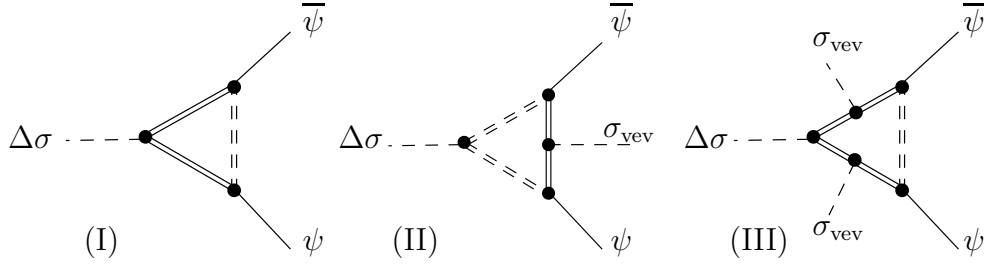
Figure 4.1: Diagrammatical interpretation of the contributions to the flow of $\overline{h}_k$.

Multiplying (4.14) and (4.16) and cubing the resulting operator is tedious, but straightforward.[8] After performing the projection rule and the trace over the inner indices,[9] we end up with

$$
\partial_t \overline{h}_k = -i \int \frac{d^d p}{(2\pi)^d} \tilde{\partial}_t \Bigg\{
$$

$$
(I) \qquad (i\overline{h}_k)^3 \frac{1}{Z_{\sigma,k}\, P(p) + U_k''(\sigma_{\mathrm{vev},k})} \frac{1}{Z_{\psi,k}^2\, P_F(p) + \overline{h}_k^2\, \sigma_{\mathrm{vev},k}^2}
$$

$$
(II) \qquad -(i\overline{h}_k)^3 \frac{\sigma_{\mathrm{vev},k}\, U_k'''(\sigma_{\mathrm{vev},k})}{\left[Z_{\sigma,k}\, P(p) + U_k''(\sigma_{\mathrm{vev},k})\right]^2} \frac{1}{Z_{\psi,k}^2\, P_F(p) + \overline{h}_k^2\, \sigma_{\mathrm{vev},k}^2}
$$

$$
(III) \qquad +(i\overline{h}_k)^5 \frac{2\,\sigma_{\mathrm{vev},k}^2}{Z_{\sigma,k}\, P(p) + U_k''(\sigma_{\mathrm{vev},k})} \frac{1}{\left[Z_{\psi,k}^2\, P_F(p) + \overline{h}_k^2\, \sigma_{\mathrm{vev},k}^2\right]^2} \Bigg\}.
$$

We can interpret the three contributions to the flow of $\overline{h}_k$ diagrammatically, as shown in Figure 4.1. Be aware that those diagrams are not to be mixed up with the common Feynman diagrams used in perturbation theory: we are not expanding in a small coupling; the propagators in our diagrams denote the full propagators (though truncated), not the classical ones.

For our final result, we consider the flow of $\overline{h}_k^2$ instead of the flow of $\overline{h}_k$ itself, using $\partial_t \overline{h}_k^2 = 2\overline{h}_k \left(\partial_t \overline{h}_k\right)$. This makes manifest that our flow equation only depends on $\overline{h}_k^2$. Again, we use a compact notation by introducing threshold functions, and switch to the dimensionless, renormalized quantities $h_k^2 =$

---

[8]One can simplifiy ones life by systematically neglecting terms that contain a field more than once.

[9]We can also neglect terms that are linear in the momentum p, as their contributions vanish under the integral due to the symmetry of the propagators.

$Z_\sigma^{-1} \, Z_\psi^{-2} \, k^{d-4} \, \overline{h}_k^2$, $u_k = U_k \, k^{-d}$ and $\kappa_k = \frac{1}{2} \, Z_\sigma \, k^{2-d} \, \sigma_{\mathrm{vev},k}^2$. Then, we get

$$
\begin{aligned}
\partial_t \, h_k^2 \;=\;& [\eta_\sigma + 2 \, \eta_\psi + d - 4] \, h_k^2 \\
& + 8 \, h_k^4 \, v_d \, l_{1,1}^{(FB)\,d} \, (\omega_1, \omega_2; \eta_\psi, \eta_\sigma) \\
& - \left[48 \, \kappa_k \, u_k''(\kappa_k) + 32 \, \kappa_k^2 \, u_k'''(\kappa_k) \right] \, h_k^4 \, v_d \, l_{1,2}^{(FB)\,d} \, (\omega_1, \omega_2; \eta_\psi, \eta_\sigma) \\
& - 32 \, h_k^6 \, \kappa_k \, v_d \, l_{2,1}^{(FB)\,d} \, (\omega_1, \omega_2; \eta_\psi, \eta_\sigma) \,,
\end{aligned}
\tag{4.17}
$$

with

$$
\begin{aligned}
\omega_1 \;&=\; 2 \, \kappa_k \, h_k^2 \\
\omega_2 \;&=\; u_k'(\kappa_k) + 2\kappa_k u_k''(\kappa_k) \,.
\end{aligned}
$$

The definitions of the threshold functions and of v_d can be found in Appendix A. Primes denote derivatives with respect to $\tilde{\rho} = \frac{1}{2} \, Z_\sigma \, k^{2-d} \, \sigma^2$, and the anomalous dimensions are defined as before: $\eta_\sigma = -\partial_t \ln Z_{\sigma,k}$ and $\eta_\psi = -\partial_t \ln Z_{\psi,k}$.

We emphasize that (4.17) differs from literature, where the same model with the same truncation was investigated in a different physical context [26]. This is due to the two additional contributions on the RHS of (4.17) that only show up at a non-vanishing vacuum expectation value.

4.4 Anomalous dimensions

Finally, we close our set of equations by deriving the flow equations for the field strength renormalizations Z_σ and Z_ψ. It will turn out to be possible to completely eliminate all explicit appearance of the field renormalizations by introducing renormalized quantities and the anomalous dimensions, as we did already before. The resulting equations will be purely algebraic, therefore saving us from having to state initial conditions; in other words: the field renormalizations influence the flow of all the other (renormalized) quantities only via the anomalous dimensions, and those are at each scale completely determined by the latter.

Anomalous dimension of the scalar As usual, we begin the derivation of the flow equation for the scalar field renormalization Z_σ by stating the

projection rule onto the operator $(\partial \sigma)^2$:

$$Z_{\sigma,k} = \frac{\partial}{\partial(p'^2)} \frac{\delta}{\delta\Delta\sigma(p')} \frac{\delta}{\delta\Delta\sigma(q')} \Gamma_k \bigg| \begin{matrix} \Delta\sigma = \psi = \overline{\psi} = 0 \\ p' = q' = 0 \end{matrix} .$$

Note that we formulate the projection rule with respect to $\Delta\sigma$ rather than $\sigma = \sigma_{\mathrm{vev}} + \Delta\sigma$. Speaking in terms of σ, this means that we allow for all operators of the form $\sigma^n(\partial\sigma)^2$ to contribute to the flow of Z_σ, as operators of the form $\sigma_{\mathrm{vev}}^n(\partial\Delta\sigma)^2$ survive the projection rule. Thus, $(\partial\sigma)^2$ and $(\partial\Delta\sigma)^2$ flow differently. As in the derivation of the flow of the Yukawa coupling, we favor the formulation with respect to $\Delta\sigma$, because in the broken regime the fluctuations relative to the vacuum expectation value constitute the dynamically relevant degrees of freedom.

With (3.2), we get for the flow equation

$$\partial_t Z_{\sigma,k} =$$

$$= \frac{1}{2} \frac{\partial}{\partial(p'^2)} \frac{\delta}{\delta\Delta\sigma(p')} \frac{\delta}{\delta\Delta\sigma(q')} \mathrm{STr} \left[\left(\partial_t R_k \right) \left(\Gamma_k^{(2)} + R_k \right)^{-1} \right] \bigg| \begin{matrix} \Delta\sigma = \psi = \overline{\psi} = 0 \\ p' = q' = 0 \end{matrix}$$

$$= \frac{1}{2} \frac{\partial}{\partial(p'^2)} \frac{\delta}{\delta\Delta\sigma(p')} \frac{\delta}{\delta\Delta\sigma(q')} \mathrm{STr} \left[\tilde{\partial}_t \ln \left(\Gamma_k^{(2)} + R_k \right) \right] \bigg| \begin{matrix} \Delta\sigma = \psi = \overline{\psi} = 0 \\ p' = q' = 0 \end{matrix} .$$

Analogous to the derivation of the flow equation for the Yukawa coupling, we decompose the operator $\left(\Gamma_k^{(2)} + R_k \right)$ into its propagator and field part according to (4.12). We get exactly the same matrices for $\left(\Gamma_{k,0}^{(2)} + R_k \right)$ and $\Delta\Gamma_k^{(2)}$ as in (4.13) and (4.14).[10] This time, we only have to consider the quadratic expansion term of the logarithm, since all the others would not

---

[10]Actually, this is not absolutely correct: Strictly speaking, we would have to include the quadratic expansion term in $\Delta\sigma$ in (4.15), as this term survives the functional derivatives within the linear expansion term of the logarithm $\ln \left\{ 1 + \left(\Gamma_{k,0}^{(2)} + R_k \right)^{-1} \Delta\Gamma_k^{(2)} \right\}$; but as the corresponding diagram is a tadpole, the loop is independent of the external momentum. And since the scalar potential, which provides the vertex to this contribution, is also momentum independent, the contribution is annihilated by the derivative with respect to p'^2.

survive the projection. Thus, our projection rule simplifies to

$$\partial_t Z_{\sigma,k} =$$

$$= -\frac{1}{4} \frac{\partial}{\partial(p'^2)} \frac{\delta}{\delta\Delta\sigma(p')} \frac{\delta}{\delta\Delta\sigma(q')} \mathrm{STr} \left[\tilde{\partial}_t \left\{ \left(\Gamma_k^{(2)} + R_k \right)^{-1} \Delta\Gamma_k^{(2)} \right\}^2 \right] \Bigg|_{\substack{\Delta\sigma=0 \\ \psi=\overline{\psi}=0 \\ p'=q'=0}} \, .$$

The matrix multiplications are quickly done when taking advantage of the vanishing fermion fields, which can be implemented right from the start, as we do not take derivatives with respect to them. After performing the traces over the inner indices and taking the functional derivatives with respect to σ, we expand the remaining integrand in p' up to second order, since only the term proportional to p'^2 is relevant for our projection. We get

$$\partial_t Z_{\sigma,k} =$$

$$= \frac{1}{d} \int \frac{d^d p}{(2\pi)^d} \, \tilde{\partial}_t \left\{ Z_{\sigma,k}^2 \, \left[U_k'''(\sigma_{\mathrm{vev},k}) \right]^2 p^2 \left(\frac{\left(\frac{\partial}{\partial p^2} P(p) \right)}{\left[Z_{\sigma,k} P(p) + U_k''(\sigma_{\mathrm{vev},k}) \right]^2} \right)^2 \right.$$

$$+ 2 \, d_\gamma \, \overline{h}_k^2 \left[p^4 \left(\frac{\partial}{\partial p^2} \frac{Z_{\psi,k} \left(1 + r_{kF}(p) \right)}{Z_{\psi,k}^2 \, P_F(p) + \overline{h}_k^2 \, \sigma_{\mathrm{vev},k}^2} \right)^2 \right.$$

$$\left. \left. - \overline{h}_k^2 \, \sigma_{\mathrm{vev},k}^2 \, p^2 \left(\frac{\partial}{\partial p^2} \frac{1}{Z_{\psi,k}^2 \, P_F(p) + \overline{h}_k^2 \, \sigma_{\mathrm{vev},k}^2} \right)^2 \right] \right\} \, .$$

In our usual dimensionless quantities and introducing threshold functions, this reads

$$\eta_{\sigma,k} = 8 \frac{v_d}{d} \left\{ \kappa_k \left[3 \, u_k''(\kappa_k) + 2 \, \kappa_k \, u_k'''(\kappa_k) \right]^2 m_{4,0}^d \left(2 \, \kappa_k \, u_k''(\kappa_k) + u_k'(\kappa_k), 0; \eta_\sigma \right) \right.$$

$$+ d_\gamma \, h_k^2 \left[m_4^{(F)\,d} \left(2 \, \kappa_k \, h_k^2; \eta_\psi \right) \right. \tag{4.18}$$

$$\left. \left. - 2 \, \kappa_k \, h_k^2 \, m_2^{(F)\,d} \left(2 \, \kappa_k \, h_k^2; \eta_\psi \right) \right] \right\},$$

where we used that $\eta_{\sigma,k} = -\partial_t \ln Z_{\sigma,k} = -\frac{1}{Z_{\sigma,k}} \partial_t Z_{\sigma,k}$. The definitions of the threshold functions can be found in Appendix A. Primes denote derivatives with respect to $\tilde{\rho}$.

40

Anomalous dimension of the fermion   The derivation of the flow equation for the fermionic anomalous dimension η_ψ follows exactly the same line of arguments as the derivation of the flow equation for the scalar anomalous dimension: The projection onto $\overline{\psi}\slashed{q}\psi$ is given by

$$
Z_{\psi,k} = \frac{1}{4d_\gamma}\operatorname{tr}\gamma^\mu\frac{\partial}{\partial p'^\mu}\frac{\overrightarrow{\delta}}{\delta\overline{\psi}(p')}\Gamma_k\frac{\overleftarrow{\delta}}{\delta\psi(q')}\bigg|_{\substack{\Delta\sigma=\psi=\overline{\psi}=0 \\ p'=q'=0}},
$$

and according to (3.2), the projected flow equation reads

$$
\partial_t Z_{\psi,k} =
$$

$$
= \frac{1}{8d_\gamma}\operatorname{tr}\gamma^\mu\frac{\partial}{\partial p'^\mu}\frac{\overrightarrow{\delta}}{\delta\overline{\psi}(p')}\operatorname{STr}\left\{\left(\partial_t R_k\right)\left(\Gamma_k^{(2)}+R_k\right)^{-1}\right\}\frac{\overleftarrow{\delta}}{\delta\psi(q')}\Bigg|_{\substack{\Delta\sigma=0 \\ \psi=\overline{\psi}=0 \\ p'=q'=0}}
$$

$$
= \frac{1}{8d_\gamma}\operatorname{tr}\gamma^\mu\frac{\partial}{\partial p'^\mu}\frac{\overrightarrow{\delta}}{\delta\overline{\psi}(p')}\operatorname{STr}\left\{\tilde{\partial}_t\,\ln\left(\Gamma_k^{(2)}+R_k\right)\right\}\frac{\overleftarrow{\delta}}{\delta\psi(q')}\Bigg|_{\substack{\Delta\sigma=\psi=\overline{\psi}=0 \\ p'=q'=0}}
$$

$$
= -\frac{1}{16d_\gamma}\operatorname{tr}\gamma^\mu\frac{\partial}{\partial p'^\mu}\frac{\overrightarrow{\delta}}{\delta\overline{\psi}(p')}\operatorname{STr}\left\{\tilde{\partial}_t\left[\left(\Gamma_{k,0}^{(2)}+R_k\right)^{-1}\Delta\Gamma_k^{(2)}\right]^2\right\}\frac{\overleftarrow{\delta}}{\delta\psi(q')}\Bigg|_{\substack{\Delta\sigma=0 \\ \psi=\overline{\psi}=0 \\ p'=q'=0}},
$$

where we employed exactly the same decomposition into a propagator and a field part, also only having to keep the quadratic expansion term of the logarithm. After performing the traces, taking the functional derivatives and expanding the integrand with respect to the external momentum p' up to first order, we find

$$
\partial_t Z_{\psi,k} = \frac{2}{d}\,\overline{h}_k^2\int\frac{d^d p}{(2\pi)^d}\,p^2
$$

$$
\times\tilde{\partial}_t\left\{\frac{Z_{\psi,k}\left(1+r_{kF}(p)\right)}{Z_{\psi,k}^2\,P_F(p)+\overline{h}_k^2\,\sigma_{\mathrm{vev},k}^2}\,\frac{Z_{\sigma,k}\left(\frac{\partial}{\partial p^2}P(p)\right)}{\left[Z_{\sigma,k}\,P(p)+U_k''(\sigma_{\mathrm{vev},k})\right]^2}\right\},
$$

which reads in dimensionless form

$$
\eta_{\psi,k} = 8\,h_k^2\,\frac{v_d}{d}\,m_{1,2}^{(FB)\,d}\left(2\,\kappa_k\,h_k^2,\,2\,\kappa_k\,u_k''(\kappa_k)+u_k'(\kappa_k);\eta_\psi,\eta_\sigma\right). \tag{4.19}
$$

41

The definition of the threshold function can be found in Appendix A. Primes denote derivatives with respect to $\tilde{\rho}$.

Chapter 5

Numerical implementation

We now have the equations at hand that we want to use to deal with our issue. But despite of the various approximations that we have already made so far, this set of equations is still too complex to be handled analytically. The reason lies in the fact that we still have to deal with an infinite number of degrees of freedom, as each value of $\tilde{\rho}$ constitutes a distinct degree of freedom of the potential. More technically speaking, (4.11) is a complicated partial differential equation, and we do not have a tool to solve it exactly. That is why our objective must be to reduce the degrees of freedom to a finite number, therewith boiling our original set of equations down to a set of finitely many coupled ordinary differential equations. Now this can be done in various ways. Most common and obvious would be just to Taylor expand the potential $u(\tilde{\rho})$ up to a finite order and then considering the flow of these finitely many expansion coefficients, neglecting the influence of higher-order coefficients. Of course, this can only be a good approximation of the potential in the vicinity of the expansion point. The flow of the expansion coefficients taken into consideration would be accurate as long as it can be guaranteed that the neglected higher-order coefficients remain small. This may be the case in perturbation theory, but we explicitly intend to extend our investigations into the non-perturbative regime. Moreover, the Taylor expansion can have unsatisfactory convergence properties, such as a finite radius of convergence in $\tilde{\rho}$ and insufficient stability.[1] Since we are especially

---

[1] In fact, for Ising-like systems the resulting expansion of the integrated potential is an asymptotic expansion.

interested in the position and shape of the potential minimum,[2] which in general must not be expected to be located close to the origin, we need a method that grasps the potential globally.

5.1 Boxing the potential

The first hurdle we have to take is to make the whole potential $u(\tilde{\rho})$ from $0 \leq \tilde{\rho} < \infty$ acessible to a finite number of degrees of freedom. It is clear that this cannot be achieved by applying an approximation technique to $u(\tilde{\rho})$ itself. We somehow have to compress the $\tilde{\rho}$ axis of infinite range to finite range. For this purpose we impose the following transformation rule:

$$r = 1 - e^{-\beta\tilde{\rho}}, \tag{5.1}$$

where we denoted the transformed field variable by r, which reaches from 0 to 1. For similar reasons, as we want to record the asymptotics of the potential, which grows towards infinity for increasing $\tilde{\rho}$, we also have to map the value of the potential itself onto a finite range. This is achieved by

$$v = \tanh(\alpha\,\hat{u}), \tag{5.2}$$

where $\hat{u} = u(\rho) - u(0)$; the use of the subtraction $u(0)$ will be explained below. The transformed potential v reaches from -1 to 1. α and β are transformation parameters, which we can choose such that the physically relevant information of the potential, for example the vacuum expectation value, is reflected optimally. The transformation rules are depicted in Figure 5.1 for various choices of α and β. The transformed flow equation for the potential v can be found in Appendix B.

5.2 Chebyshev approximation

Next, we have to find an appropriate way of approximating the boxed potential. Our guidelines are given by the requirements of fast convergence, simple computation and that the approximation be global, meaning: no expansion around a single point, but embracing information across the whole range of r.

---

[2]Because those carry the relevant information on the vacuum expectation value and the Higgs mass.
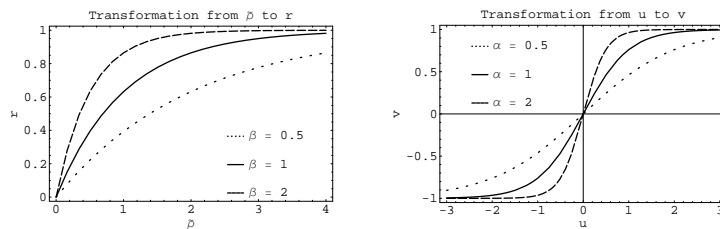
Figure 5.1: "Boxing" transformations of the field variable $\tilde{\rho}$ and the potential u

More technically, we need to interpolate the potential. We decided to choose a special polynomial interpolation technique, the Chebyshev approximation. The Chebyshev polynomials are orthonormal and complete in the interval $[-1, 1]$ over a weight $(1-x^2)^{-1/2}$. The Chebyshev approximating polynomial is distinguished by the fact that it is very close to the minimax polynomial, which, among all polynomials of the same degree, has the smallest maximum deviation from the true function. But while the minimax polynomial is very difficult to find, the Chebyshev polynomial is very easy to compute. More details on the definition of the Chebyshev polynomials and their explicit form can be found in Appendix C. The Chebyshev coefficients of the (truncated) Chebyshev approximation of the boxed potential now are the finitely many degrees of freedom of our concern; we will numerically determine the flow of these coefficients.

5.3   Stabilizing the flow

Though we do not want to go to much into the technical details of our implementation, we nevertheless think that some remarks are in place. As we intend to have our system flow over many scales, it must be expected that also the potential experiences changes of the order of several scales. This is most obvious for the relevant components, which even grow exponentially with the logarithmic scale variable $t = \ln k/\Lambda$. But also the marginal components can cause a remarkable change, if the flow goes over many scales. Numerically this poses a huge problem, as the large numbers "swallow" the small ones, which often carry the more important physical information. We somehow have to make arrangements in order to limit the range of scales the potential undergoes. More concretely, we want the flow to be dominated by the physics

relevant to us, and not by some "rubbish" we are not interested in.

Eliminating the cosmological constant   We have already done a first step by considering the dimensionless flow; the canonical scaling induced by the running scale k, which we used in order to make all quantities dimensionless, should at least partially compensate the flow due to strong radiative corrections. This is especially obvious for the dimensionless mass parameter m_k^2/k^2, which we fine-tune such that it remains small over many scales. But still we have to expect that the most divergent quantity, the cosmological constant, grows sufficiently strong to spoil our numerics. We solve this problem by realizing that the cosmological constant does not at all play any role with respect to the physics we are interested in, because it does not influence the flow of all the other operators, which contain the information on the vacuum expectation value, the Higgs mass and so on. This is why we immediately implement, as a second precaution, the flow of the difference $u_k(\tilde{\rho}) - u_k(0)$ (or rather its transformed version) instead of the flow of $u_k(\tilde{\rho})$ itself. On the one hand, we ignore the flow of the cosmological constant in this way, on the other hand we protect our flow from its huge growth and its capability to spoil our results.

Switching to fixed-scale flow   As mentioned above, we fine-tune the dimensionless mass parameter such that it remains small over many scales. When eventually the dimensionless mass parameter becomes of the order of one, this means that the integration scale k is passing the mass and fluctuations cease to drive the flow, since then the natural mass scale of the theory acts as an IR cut-off. During the freeze-out process the dimensionless mass parameter and its subsequent exponential growth starts to dominate the flow more and more, which becomes numerically problematic. We handle this problem by realizing that the absence of fluctuations allows us to safely switch back to the fixed-scale flow equation, which we then solve in units of a suitable fixed scale; in practice, we use the scale at which we switch from the dimensionless flow to the fixed-scale flow. Of course, this fixed scale is completely auxiliary and physical scales are independent of this scale. Within the fixed-scale flow all couplings come to a halt, resulting in a well-balanced numerical result.

46

Adjusting the transformation parameters α and β   After having solved the most urgent problems, we still have to consider that even the marginal couplings can undergo a significant change when integrating over many scales. In particular, this will occur in the limiting cases of large, non-perturbative cut-off couplings, or when the ϕ^4 coupling at the cut-off is several scales smaller than the Yukawa coupling.[3] In order to prevent that the physics is pushed towards the edges of the box, where the resolution is bad, we make use of the freedom to choose the transformation parameters α and β (see (5.1), (5.2)). We adjust them in the course of the flow such that the physically interesting regions of the potential are at each instant rendered optimally within the box.

Fine-tuning the mass parameter   One more remark on the fine-tuning of the mass parameter: in principle we could fine-tune the component of the the dimensionless mass parameter proportional to k^{-2} to such precision,[4] that we could get a flow over as many scales as we want to, before the freeze-out. Practically, the range of our fine-tuning is restricted by our numerical accuracy, in particular that of the floating point arithmetic. At some point the required fine-tuning becomes more subtle than the floating point resolution of our machine, and a change of the mass parameter does not result in an increase of the range of the flow anymore. We find that with optimum fine-tuning we get as far as six integration scales, which is by no means enough for our purpose. We solve this problem by adding every several scales a small correction mass to the current potential, which is supposed to undo the growth of the tuning parameter.

$$u_{k,\text{new}}(\tilde\rho) = u_{k,\text{old}}(\tilde\rho) + a_{\text{correction}}\,\tilde\rho. \tag{5.3}$$

As long as this correction mass is small enough, the influence on the flow of all the other couplings will be negligible. We want to stress that we also do not tamper with the flow of the dimensionless mass parameter itself: by

---

[3]We will restrict our investigation to a quartic cut-off potential. This will be justified in some detail in Chapter 7.

[4]We can think of the dimensionless mass parameter in an expansion in k. Its relevant nature then is reflected by the occurence of a term proportional to k^{-2}, which yields an exponential growth in the logarithmic scale variable $t = \ln k/\Lambda$. By suitably choosing the cut-off mass m_Λ, the coefficient of this term in principle can be made arbitrarily small; this corresponds to fine-tuning.

expansion of (4.11) (and assuming a linear cut-off function), we get the flow equation for the dimensionless mass parameter:

$$
\begin{aligned}
\partial_t u_k'(0) \;=\; & \frac{8\, h_k^2\, d_\gamma\, v_d}{d}\left(1 - \frac{\eta_\psi}{1+d}\right) \\
& + (\eta_\sigma - 2)\, u_k'(0) \\
& + \frac{12\, v_d\, u_k''(0)}{d(1 + u_k'(0))^2}\left(\frac{\eta_\sigma}{2+d} - 1\right).
\end{aligned}
\tag{5.4}
$$

Inspecting (5.4), we see that the first term on the RHS does not depend on the current value of u_k' and the third only to higher order, being insensitive to small corrections. Thus, only the median term is noticeably affected by the additive mass term. But this term just reflects the exponential growth of the dimensionless mass parameter due to the non-vanishing tuning parameter. Therefore, adding the small mass correction corresponds to retuning the original tuning parameter. In other words, backtracking the influence of the mass correction on the cut-off dimensionless mass parameter, we find that due to the irrelevant character of the flow in this direction the modification is much smaller than the original mass correction and occurs far behind the leading digit, which justifies to consider it as a fine-tuning in first place.

Chapter 6

Simple applications and benchmark tests

In order to test our approach (and our implementation), we apply it to situations, in which we know the behaviour of the system analytically, at least in some limiting cases. Namely, those are the scaling potential for a scalar theory due to the Wilson-Fisher fixed point in three dimensions and the renormalisation group flow of our Toy Model truncation in the vicinity of the Gaussian fixed point in four dimensions. However, we want to emphasize that our approach can go far beyond those analytic results, especially in the three-dimensional case we are able to give a global approximation to the scaling potential [1], whereas analytically only a local approximation in the limiting cases of small and large ρ can be made. But this is not of primary interest in this work. In the four-dimensional case, the behavior of the Toy Model away from the Gaussian fixed point will, of course, be a major point of investigation in the remainder of this work.

6.1 Recovering the 3D scaling potential due to the Wilson-Fisher fixed point

As is well known, the pure scalar theory exhibits two scaling solutions in $2 < d < 4$ dimensions, which correspond to the Gaussian and the Wilson-

---

[1]At this, it must not be forgotten that the form of the scaling potential is regulator dependent.

Fisher fixed point, respectively [27]. This property is still maintained when restricting oneself to the local potential approximation, which is given by the truncation

$$\Gamma_k = \int d^d x \left(\frac{1}{2} \partial_\mu \sigma \, \partial^\mu \sigma + U_k(\rho) \right), \tag{6.1}$$

where $\rho = \frac{1}{2}\sigma^2$. Actually, this investigation can easily be generalised to the case of an $O(N)$ symmetric scalar theory, but as we are only interested in a single scalar field, we restrict ourselves to the present case.

It can easily be seen that this truncation is identical to our Toy Model truncation when neglecting the Yukawa coupling and the scalar field renormalization. The local potential approximation, interpreted as a derivative expansion to leading order, can be justified by taking into consideration that the neglected higher-order corrections are proportional to the anomalous dimension η, which is small in our case. As the truncation of our Toy Model respects the scalar field renormalization, we can explicitly verify the smallness of the anomalous dimension (see below).

In order to be able to derive the form of the scaling potential analytically, at least in the limiting cases of small and large field strength, we now determine the renormalization flow equation for the effective average potential following from the local potential approximation. This, of course, will be performed by applying the ERGE scheme to the truncation above. Evaluating the resulting flow equation of the effective average action for constant field ($\sigma = $ const), we end up with the flow equation for the effective average potential

$$\partial_t u + du - (d-2)\tilde{\rho} u' = 2 v_d \, l(2\tilde{\rho} u''), \tag{6.2}$$

which we have formulated in the dimensionless quantities $\tilde{\rho} = \frac{1}{2}\sigma^2 k^{2-d}$ and $u(\tilde{\rho}) = U_k/k^d$ ($v_d^{-1} = 2^{d+1} \pi^{d/2} \Gamma(\frac{d}{2})$). The function $l(\omega)$ is given by

$$l(\omega) = \frac{1}{2} \int_0^\infty dy \, y^{d/2} \frac{\partial_t r(y)}{y(1+r) + \omega} \tag{6.3}$$

with $y = q^2/k^2$ and $R(q^2) = q^2 r(q^2/k^2)$.

Now we choose as regulator a linear cut-off function, given by

$$r(y) = \left(\frac{1}{y} - 1 \right) \Theta(1 - y), \tag{6.4}$$

which is optimized in the sense that it leads to the most rapid convergence and the highest stability of an approximated flow towards the physical theory

50

[25]. Note that for approximated flows not only the trajectory but also the end point of the flow depends on the regulator. Evaluating (6.2) using this regulator yields the flow equation

$$\partial_t u = -du + (d-2)\tilde{\rho}u' + \frac{4}{d}v_d \frac{1}{1 + u' + 2\tilde{\rho}u''}. \qquad (6.5)$$

Finally, as we are only interested in the scaling potential, which is defined as being invariant under the renormalization group transformation, we can set the RHS equal to zero. Furthermore, we confine ourselves to the case of three dimensions:

$$0 = -3u_* + \rho u'_* + \frac{1}{6\pi^2} \frac{1}{1 + u'_* + 2\tilde{\rho}u''_*}. \qquad (6.6)$$

We are interested in non-trivial solutions of this differential equation.

Polynomial approximation at the origin   As we still cannot solve equation (6.6) exactly, we have to look for ways to get at least approximate solutions to it. One possibility is of course a (truncated) Taylor expansion in the vicinity of the origin. Inserting the ansatz

$$u(\tilde{\rho}) = \sum_{n=0}^{n_{\text{trunc}}} \frac{1}{n!}\lambda_n \tilde{\rho}^n \qquad (6.7)$$

into (6.6), the differential equation is transformed into n_{trunc} coupled equations for the set of couplings $\{\lambda_n, 0 \le n \le n_{\text{trunc}}\}$. As we have only n_{trunc} equations for $n_{\text{trunc}} + 1$ unknowns, we are left with one parameter, which we choose to be λ_1 (dimensionless mass term at vanishing field). Solving this system of equations, we get

$$
\begin{aligned}
\lambda_0 &= \frac{1}{18\pi^2}(1 + \lambda_1)^{-1} \\
\lambda_2 &= -4\pi^2\lambda_1(1 + \lambda_1)^2 \\
\lambda_3 &= \frac{72}{15}\pi^4\lambda_1(1 + \lambda_1)^3(1 + 13\lambda_1) \\
\lambda_4 &= -\frac{1728}{7}\pi^6\lambda_1^2(1 + \lambda_1)^4(1 + 7\lambda_1) \\
\lambda_5 &= \frac{768}{7}\pi^8\lambda_1^2(1 + \lambda_1)^5(2 + 121\lambda_1 + 623\lambda_1^2). \\
&\vdots
\end{aligned}
\qquad (6.8)
$$

51

The value for λ_1, which corresponds to the Wilson-Fisher fixed point, is determined by fine tuning λ_1 such that the solution (6.8) reaches its maximum radius of convergence. We find $\lambda_{1*} = -0.186...$ in agreement with [25].

Asymptotic behaviour for large $\tilde{\rho}$ In the other limit, for large fields, $\tilde{\rho} \gg 1$, we can neglect in a first approximation the third term on the RHS of (6.6) and find by a simple separation of variables that

$$u_*(\tilde{\rho}) = A\,\tilde{\rho}^3, \tag{6.9}$$

with $A > 0$. The latter condition follows already from the requirement of stability, that any sensible physical potential has to fulfill.

Comparison with numerical results   Now that we have determined the scaling potential in the limiting cases of small and large $\tilde{\rho}$, we can use those analytic results in order to test our numerics.[2] We have to choose a starting potential u_Λ at the cut-off, which is in the universality class of the Wilson-Fisher fixed point. As we do neither know the coordinates of the Wilson-Fisher fixed point in "theory space" nor its universality class, we cannot a priori determine such a starting potential, but only verify properties characteristic for the Wilson-Fisher fixed point for a more or less arbitrarily chosen starting potential. In addition, one parameter of the starting potential has to be fine-tuned, as the Wilson-Fisher fixed point exhibits one relevant eigendirection. The fine-tuning guarantees that the RG trajectory passes close to the fixed point and therefore stays there over many scale integrations, such that the fixed-point scaling behavior in the RG flow can be identified, yielding the scaling potential. A cut-off potential fulfilling all those requirements is given by

$$u_\Lambda(\tilde{\rho}) = a\,\tilde{\rho} + 0.5\,\tilde{\rho}^2 \tag{6.10}$$

with a fine-tuned at $a = -0.040...$. We emphasize that the value of the fine tuning parameter is not universal, but depends also on the regulator and is sensitive to the numerical accuracy, the chosen step width, the transformation parameters α and β,...; that is why we have only given the leading digits,

---

[2]In order to be able to compare the results of our approach best with the analytically gained results, we neglect in our numerics the scalar field renormalization in this part of the investigation, to match the local potential approximation; but for a later prediciton of the anomalous dimension η_σ, we will take it into account, again.
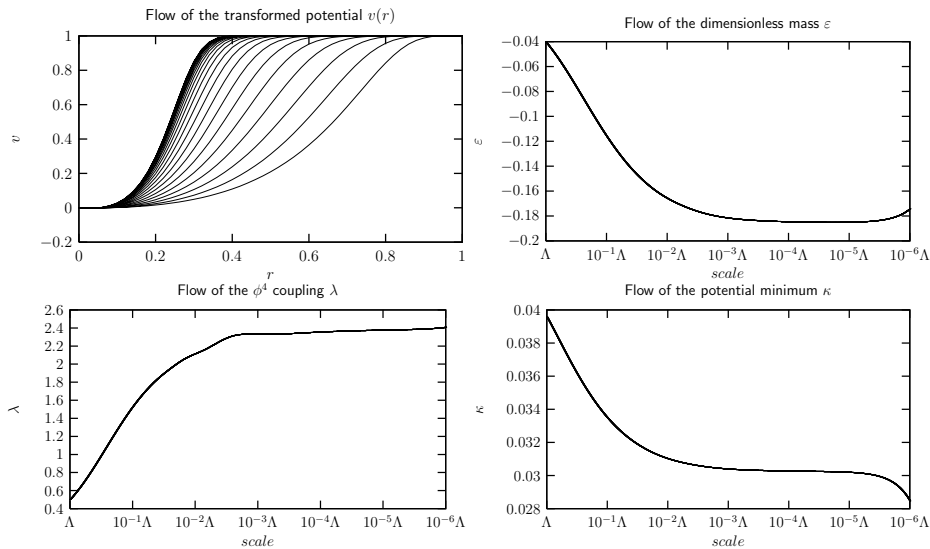
Figure 6.1: RG flow in the vicinity of the Wilson-Fisher fixed point. The top-left plot gives snapshots of the potential flow, approaching the fixed-point potential from right to left.

to provide an intuition for the order of magnitude: this choice of the tuning parameter yields a minimum of the potential at about $\rho \approx 0.04$, which in turn corresponds to a minimum in the transformed potential at $r \approx 0.04$ for $\alpha = \beta = 1$. As we restrict ourselves to a pure scalar theory, the cut-off Yukawa coupling is, of course, set to zero: $h_\Lambda^2 = 0$, and therewith the effective Yukawa coupling throughout the flow, too.

The flow resulting from the starting potential (6.10) is displayed in Figure 6.1. It can be seen very nicely that the flow approaches a (non-Gaussian) fixed point and stays very close to it over several scales, before it is pushed away by the relevant component, again. We take the potential that is reached after four scales of integration as our approximation to the scaling potential. We want to compare the form of this potential to the analytic results derived above.

Taking the data in the vicinity of the origin, transforming it back to the original parametrisation $u(\tilde{\rho})$ and interpolating it, we can compare it to the prediction of the Taylor approximation derived above. The result given in Figure 6.2 shows that both approaches match perfectly, which gives us a great deal of confidence that our approach is capable to reproduce even "subtle"
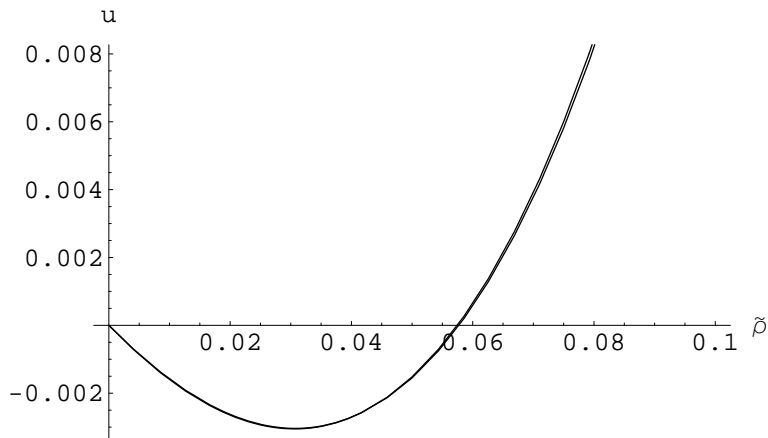
Figure 6.2: Comparison of the Taylor-approximated scaling potential to our numerical result (it's two lines!). This curve solves eq (6.6).

details of the (exact) flow. This is particularly remarkable, since the minimum of the potential is very shallow compared to the complete "boxed" potential; its modulus amounts to only two permille of the height of the boxed potential.

Next, we also want to check, if our approach yields the correct asymptotic behaviour for large $\tilde{\rho}$, which we derived to be proportional to $\tilde{\rho}^3$. By fitting our data to the transformed version of the Ansatz $a\,\tilde{\rho}^b$ (a and b being the fitting parameters), we get $b = 3.03$ (a is not of interest here), which, again, matches satisfactorily with the analytic prediction. The minor discrepancy can be attributed to the fact that our data also reflects the region of small $\tilde{\rho}$, where the approximation made to derive the asymptotic behaviour does not hold anymore.

Finally, we can check, if we are able to reproduce the anomalous dimension η_σ, as it is predicted by our truncation: $\eta_\sigma = 0.1147$ [3] [24]. As up till now we neglected the influence of the scalar anomalous dimension on the flow of the potential, we have to fine-tune once more, this time including the flow of the scalar field renormalisation. The smallness of the predicted anomalous dimension supports the assumption that a possible cut-off potential $u_\Lambda(\tilde{\rho})$ can be found very close to (6.10), and indeed we find a flow passing closely

---

[3]We emphasize that the actual value differs significantly from this prediction of our truncation.

54
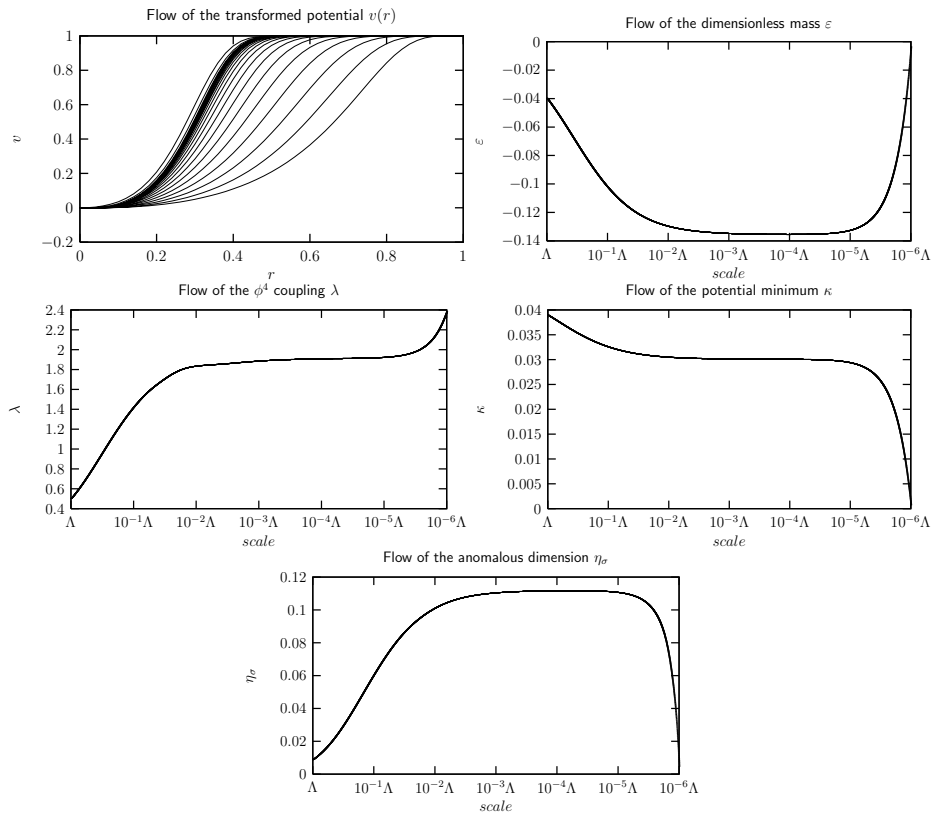
Figure 6.3: RG flow in the vicinity of the Wilson-Fisher fixed point, including the influence of the scalar field renormalization. As in Figure 6.1, the top-left plot gives snapshots of the potential flow, approaching the fixed point potential from right to left.

the Wilson-Fisher fixed point choosing $u_\Lambda(\tilde\rho) = -0.039... \tilde\rho + 0.5\, \tilde\rho^2$, as can be checked in Figure 6.3. Examining Figure 6.3, the scalar anomalous dimension in the scaling region can be read off as $\eta_\sigma = 0.11...$, which is in good agreement with the literature. The anomalous dimension is of particular interest, because critical exponents are scheme independent.

Concluding this section, we can say that so far our approach fulfilled all of our expectations. In the next section, we will extend this investigation to the case of four dimensions.

6.2   Perturbative flow in 4D

In this section, we want to test our approach in the for our purpose more relevant case of four dimensions, this time in the vicinity of the Gaussian fixed point. There, as we will show, our flow equations simplify to the results obtained in 1-loop perturbation theory, which gives us a simply opportunity to test the power of our approach at hand. A major difference between the Wilson-Fisher fixed point in 3D and the Gaussian fixed point in 4D is that, while in the first case the spectrum of eigendirections contains exactly one relevant eigenvector and besides only irrelevant, in the latter the coupling corresponding to the ϕ^4 operator[4] turns dimensionless (marginal), resulting in a logarithmic scaling behaviour (near the Gaussian fixed point dimensional arguments are permitted). This logarithmic scaling behaviour prevents the potential from rapidly converging towards its fixed point, even when the RG trajectory is fine tuned to be very close to the irrelevant submanifold. That is why we expect that in the regime of the Gaussian fixed point the couplings with negative mass dimension should die out rapidly, leaving over a ϕ^4 theory flowing logarithmically in its interaction coupling. More precisely, only the tree-level parts of the irrelevant operators should die out, leaving over the parts generated by the interactions. Since the latter are controlled by the dimensionless couplings, they should therefore be small in the perturbative limit. Again, we are mostly interested in testing the applicability of our method of treating the scalar potential. For that purpose, we have two tests at hand: First, we focus on the flow of the ϕ^4 coupling. We will show that the corresponding β function derived from our flow equation can be approximated by the well-known β function following from one-loop perturbation theory in (massless) ϕ^4 theory, which can be integrated analytically and therefore yields a basis for a comparison to our numerics. Second, we analytically solve the ERGE for the potential as a whole in mean-field approximation to first order and in the limit of an infinitely large scalar mass (meaning that only fermionic fluctuations contribute to the flow of the effective potential). This test probes the potential globally, being sensitive to all operators, including the irrelevant ones.

---

[4]Note that we are talking about ϕ^4 theory and the ϕ^4 coupling: this is just to meet conventions; of course, we still denote our classical scalar field by σ.

6.2.1 Flow of the ϕ^4 coupling

We consider the flow of our truncation in the limit of vanishing Yukawa coupling and with a perturbative starting potential u_Λ. We want to show that in this case the β function for the ϕ^4 coupling simplifies to the one-loop β function of (massless) ϕ^4 theory, which can be integrated analytically. In the course of this derivation we will have to make some assumptions, which only can be justified as being good approximations in the vicinity of the Gaussian fixed point. This is due to the fact that our flow equations also include higher-order effects, which can only be neglected in the perturbative limit. This is why we have to require the starting potential to be perturbative. Actually we could even gain exact agreement between the β functions, if we further truncated the potential to $u_k = \lambda_k \, \tilde{\rho}^2$, because all higher-order operators (in powers of $\tilde{\rho}$) are only generated by higher order effects in an expansion in λ. But this somehow would contradict the philosophy of our approach to consider the full scalar potential. And, as we will see, we get very good agreement, anyway. The scalar field renormalization, which also is a higher-order effect, we will indeed neglect, just by feeding the potential flow equation with a vanishing scalar anomalous dimension. So, effectively, we work once more in the Local Potential Approximation.

Derivation of the β function Starting with (4.11), setting $h_k = 0$ and expanding in powers of $\tilde{\rho}$, the resulting flow equation of the coefficient of the $\tilde{\rho}^2$ operator reads

$$\partial_t \lambda_k = -d\,\lambda_k + (d - 2 + \eta_\sigma)\, 2\,\lambda_k + 2\, v_d\, \frac{1}{2}\, \frac{d^2 l_0^d}{(d\tilde{\rho})^2}\Big|_{\tilde{\rho}=0}, \qquad (6.11)$$

where we take $u_k = \varepsilon_k\, \tilde{\rho} + \lambda_k\, \tilde{\rho}^2 + ...$ Inserting $d = 4$ and assuming $\eta_\sigma = 0$, which is a good approximation in the vicinity of the Gaussian fixed point, we get

$$\partial_t \lambda_k = v_4\, \frac{d^2 l_0^d}{(d\tilde{\rho})^2}\,|_{\tilde{\rho}=0}\,. \qquad (6.12)$$

Choosing a linear cut-off function given by $l_n^d(\omega) = \frac{2(\delta_{n,0}+n)}{d}(1 - \frac{\eta_\sigma}{d+2})\frac{1}{(1+\omega)^{n+1}}$, we end up with

$$\partial_t \lambda_k = v_4 \left(\frac{9\left(u_k''(\tilde{\rho}=0)\right)^2}{\left(1 + u_k'(\tilde{\rho}=0)\right)^3} - \frac{5\, u_k^{(3)}(\tilde{\rho}=0)}{2\left(1 + u_k'(\tilde{\rho}=0)\right)^2} \right). \qquad (6.13)$$

Note that the β-function is universal to one-loop order; the special choice of the regulator therefore does not mean a loss of generality as long as we stay away from mass thresholds. Now, the above mentioned assumptions on the behaviour of the potential come into play: Given a perturbative cut-off potential u_Λ that does not contain any higher-order operators beyond $\tilde{\rho}^2$ (which, being tree-level components with negative mass dimension, would rapidly die away, anyway), the $\tilde{\rho}^3$ operator is completely controlled by the ϕ^4 coupling to a leading power of λ_Λ^3. Thus, $u_k^{(3)}(\tilde{\rho} = 0)$ remains small and we can neglect its contribution to the flow of the ϕ^4 coupling. A similar argument accounts for $u'_k(\tilde{\rho} = 0)$: again, the radiative corrections to the $\tilde{\rho}$ operator are controlled by λ_Λ and thus small; the tuning parameter therefore has to be small, as well.[5] Since the cut-off mass m_Λ^2 is supposed to compensate the tuning parameter, it generically has to be small, too. Hence, $u'_k(\tilde{\rho} = 0)$ is small as long as it is well fine-tuned and we can neglect its contribution to (6.13). That is why in the vicinity of the Gaussian fixed point the flow equation simplifies to

$$\partial_t \lambda_k = 9\, v_4 \left(u''_k(0) \right)^2 = \frac{18\, \lambda_k^2}{16\, \pi^2}. \tag{6.14}$$

Within the more common definition of the ϕ^4 coupling, which differs from the present convention by a factor of $1/6$ [28], we find that we are in agreement with the textbook β function to one-loop order of (massless) ϕ^4 theory [28]

$$\partial_t \lambda_{k,\text{textbook}} = \frac{3\lambda_{k,\text{textbook}}^2}{16\pi^2}. \tag{6.15}$$

Equation (6.14) can be integrated by separation of variables to become

$$\lambda_k = \frac{\lambda_\Lambda}{1 - \frac{18\lambda_\Lambda}{16\pi^2} \ln\left(\frac{k}{\Lambda}\right)}. \tag{6.16}$$

Comparison with numerical results We determine the flow of the potential numerically starting with a perturbative cut-off potential $u_\Lambda = a\, \tilde{\rho} + 0.5\, \tilde{\rho}^2$, where a is fine-tuned such that ε_k remains small over many scales, before it starts to grow. As soon as the mass becomes important, the massless β function is no longer a good approximation and the flow eventually

---

[5]If we think of the radiative corrections to the bare mass m_Λ^2 in an expansion in k, the tuning parameter is the coefficient of the k^0 expansion term.
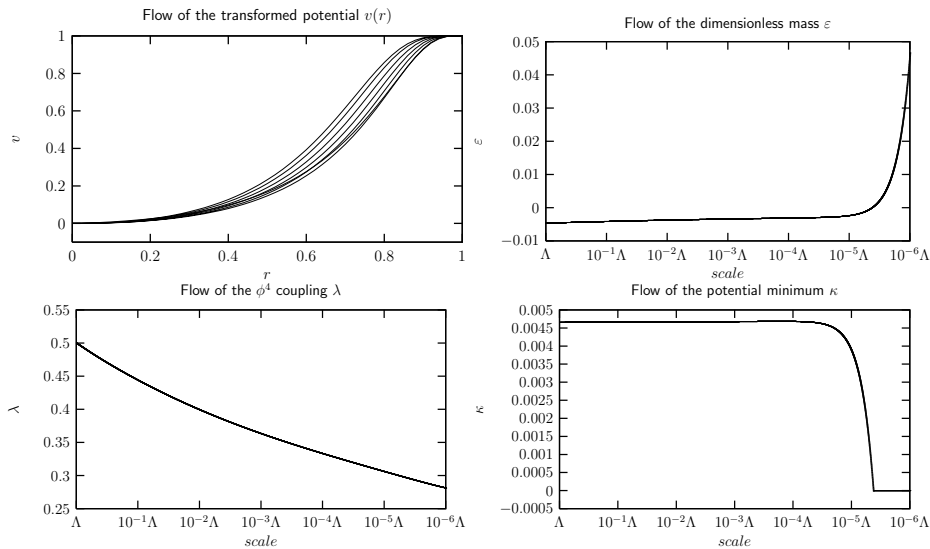
Figure 6.4: RG flow of the effective average potential in the 4D Local Potential Approximation with starting potential $u_k = -0.0004... \tilde{\rho} + 0.5 \tilde{\rho}^2$. As can be seen in the bottom-right plot, the potential starts with a vacuum expectation value, but finally ends up in the symmetric regime.

"freezes out"[6] (also remember that $h_\Lambda = 0$ and by hand $\eta_\sigma = 0$). We find that for $a = -0.004...$ ε_k remains small over six scales integration. The result of the flow can be viewed in Figure 6.4.

Finally, the comparison of the resulting numerical flow of λ_k with the predicted flow according to (6.16) is depicted in Figure 6.5. It can be stated that they are in very good agreement. So far, the implementation works fine!

6.2.2 Mean-field fermionically induced scalar potential

In this test we introduce for the first time a non-vanishing Yukawa coupling. Actually, we restrict ourselves exclusively to the effect of the Yukawa coupling on the flow of the effective average potential, meaning that we consider only the contribution of the fermionic fluctuations, leaving the scalar fluctuations aside. Formally, this is achieved by assuming an infinitely large scalar mass. We use that in this limit we can solve the ERGE for the scalar potential in mean-field approximation to first order analytically. 'Mean-field'

---

[6]I.e., the massive modes decouple in the IR.
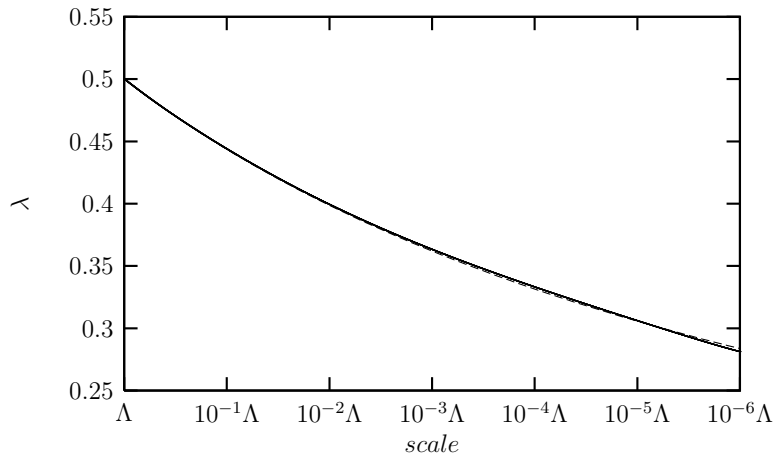
Figure 6.5: Comparison of the analytically predicted flow of the ϕ^4 coupling (solid line) with the numerically gained (dashed line).

in this context means that the (fermionic) propagator used to integrate out fluctuations is not k dependent but the classical one throughout the whole flow. By neglecting the bosonic threshold function (which takes care of the scalar fluctuations) on the RHS of (4.11), artificially keeping the Yukawa coupling constant at its cut-off value and neglecting the fermionic anomalous dimension, we should get exact agreement between the numerics and the analytical result. We want to stress that this is even true for a large Yukawa coupling, beyond the perturbative region; physically, the mean-field approximation may not be justified in this region, nevertheless, mathematically, nothing can keep us from probing our flow in this region, as the significance of the fluctuation effects grows with the Yukawa coupling. The advantage of this test is that it is sensitive to the potential as a whole, not only to a small subset of operators. As we already know that our approach is powerful in reproducing the flow of the operators with positive or vanishing mass dimensions, we use the possibility to focus now on the operators with negative mass dimension.

Analytical solution of the ERGE We want to evaluate (3.2) in mean-field approximation in the limit of vanishing fermionic "classical" fields ($\psi = \overline{\psi} = 0$) and a constant scalar classical field ($\sigma = \sigma_0 = \text{const}$), because this prescription obviously yields the flow equation for the scalar potential. By 'mean-field' we mean that the underlying propagator used to integrate out

60

the fluctuations is independently of the scale k the classical propagator (just like in standard perturbation theory). In our language, we want to evaluate the ERGE applying the following truncation:

$$\Gamma_F \;=\; \int \frac{d^d q}{(2\pi)^d}\Bigg[-\overline{\psi}(q)\slashed{q}\,\psi(q)$$
$$+ \int \frac{d^d p}{(2\pi)^d}\Big(ih_\Lambda \overline{\psi}(p)\sigma(p-q)\psi(q)\Big)\Bigg]. \tag{6.17}$$

Remember that the structure of the truncation only constitutes the form of the propagator used to integrate out fluctuations. The actual effective action at the scale k gained from the flow equation in general contains arbitrarily many operators. Therefore, the absence of the scalar potential in (6.17) does not mean that there is not generated a scalar potential. The fluctuation matrix, that follows from (6.17) (evaluated for a constant scalar background field), reads

$$\Gamma^{(2)}_{F,0}(p,q) \;=\; \left(\begin{array}{c} \frac{\overrightarrow{\delta}}{\delta\psi^T(-p)} \\[4pt] \frac{\overrightarrow{\delta}}{\delta\overline{\psi}(p)} \end{array}\right) \Gamma_k \left(\; \frac{\overleftarrow{\delta}}{\delta\psi(q)} \;,\; \frac{\overleftarrow{\delta}}{\delta\overline{\psi}^T(-q)} \;\right)\Bigg|_{\sigma=\sigma_0}$$
$$= \left(\begin{array}{cc} 0 & -\slashed{p} - ih_\Lambda\sigma_0 \\[4pt] -\slashed{p} + ih_\Lambda\sigma_0 & 0 \end{array}\right) \delta_{p,q}. \tag{6.18}$$

The flow equation for the scalar potential then reads

$$\partial_t U_{k,F} = -\frac{1}{2}\,\mathrm{Tr}\left(\frac{(\partial_t R_{F,k})}{\Gamma^{(2)}_{F,0} + R_{F,k}}\right), \tag{6.19}$$

the minus sign comes from the 'super-trace'. We can simplify (6.19) significantly by making use of the fact that $\Gamma^{(2)}_{F,0}$ does not depend on k, which allows us to exchange the trace and the derivative with respect to t (without having to introduce the operator $\tilde{\partial}_t$, which is defined to act only on the regulator), yielding

$$\partial_t U_{k,F} = -\frac{1}{2}\,\partial_t\,\mathrm{Tr}\ln\left(\Gamma^{(2)}_{F,0} + R_{F,k}\right), \tag{6.20}$$

61

which can be integrated straightforwardly:

$$
\begin{aligned}
U_{\Lambda,F} - U_{k,F} &= -\frac{1}{2} \int \frac{d^d q}{(2\pi)^d}\, \mathrm{tr}\, \ln\left(\frac{\Gamma_{F,0}^{(2)} + R_{F,\Lambda}}{\Gamma_{F,0}^{(2)} + R_{F,k}}\right) \\
&= -\frac{1}{2} \int \frac{d^d q}{(2\pi)^d}\, \mathrm{tr}\left[\ln\left(\frac{(-\slashed{q} + R_{F,\Lambda}(q) + ih_\Lambda\sigma_0)}{(-\slashed{q} + R_{F,k}(q) + ih_\Lambda\sigma_0)}\right)\right. \\
&\qquad\left. + \ln\left(\frac{\slashed{q}^T + R_{F,\Lambda}(-q) + ih_\Lambda\sigma_0}{\slashed{q}^T + R_{F,k}(-q) + ih_\Lambda\sigma_0}\right)\right].
\end{aligned}
\tag{6.21}
$$

Here we have decomposed the symbolic trace Tr into its momentum space and Dirac space parts. In the second line we have inserted (6.18) and used that Tr ln is equivalent to ln det. Now, we specify the regulator as $R_{F,k}(q) = -\slashed{q}\, r_{F,k}(q)$ with the linear cut-off function $q^2\big(1 + r_{F,k}(q)\big)^2 = q^2\big[1 + (\frac{k^2}{q^2} - 1)\Theta(1 - \frac{q^2}{k^2})\big]$. We evaluate the Dirac traces and exploit the spherical symmetry of the integrand, while setting $d = 4$. Then, we get

$$
\begin{aligned}
U_{\Lambda,F} - U_{k,F} = -\frac{1}{4\pi}\Bigg[&\int_0^\Lambda dp\, p^3 \ln\left(1 + \frac{h_\Lambda^2 \sigma_0^2}{\Lambda^2}\right) \\
&- \int_0^k dp\, p^3 \ln\left(1 + \frac{h_\Lambda^2 \sigma_0^2}{k^2}\right) \\
&- \int_k^\Lambda dp\, p^3 \ln\left(1 + \frac{h_\Lambda^2 \sigma_0^2}{p^2}\right)\Bigg].
\end{aligned}
\tag{6.22}
$$

Observe that the special choice of the regulator limits the range of integration to the cut-off Λ. Thus, the integrations can be performed without problems, and we end up with

$$
U_{k,F} = U_{\Lambda,F} + \frac{1}{16\pi^2}\left[(k^2 - \Lambda^2)\, h_\Lambda^2 \sigma_0^2 + h_\Lambda^4\, \sigma_0^4 \ln\left(\frac{\Lambda^2 + h_\Lambda^2 \sigma_0^2}{k^2 + h_\Lambda^2 \sigma_0^2}\right)\right].
\tag{6.23}
$$

Switching to the dimensionless quantities $u_k = U_k/k^4$ and $\tilde\rho = \frac{1}{2}\sigma_0^2/k^2$, our final result reads

$$
u_{k,F} = \frac{U_{\Lambda,F}}{k^4} + \frac{1}{16\pi^2}\left[2\left(1 - \frac{\Lambda^2}{k^2}\right) h_\Lambda^2 \tilde\rho + 4 h_\Lambda^4 \tilde\rho^2 \ln\left(\frac{\frac{\Lambda^2}{k^2} + 2h_\Lambda^2\tilde\rho}{1 + 2h_\Lambda^2\tilde\rho}\right)\right].
\tag{6.24}
$$

It is worth the time to analyze (6.24) in a little bit more detail. If we expand the RHS in $\tilde{\rho}$, assuming $U_{\Lambda,F} = m_\Lambda^2 \, \rho + \lambda_\Lambda \, \rho^2 + ...$, we get

$$u_{k,F} = \left(\frac{\Lambda^2}{k^2} \left[\frac{m_\Lambda^2}{\Lambda^2} - \frac{h_\Lambda^2}{8\pi^2} \right] + \frac{h_\Lambda^2}{8\pi^2} \right) \tilde{\rho} + \left(\lambda_\Lambda - \frac{h_\Lambda^4 \, \ln \frac{k}{\Lambda}}{2\pi^2} \right) \tilde{\rho}^2 + ... \qquad (6.25)$$

From this we can see two properties of the flow:

First, we realize that we have to fine-tune the term in the square brackets, if we want to keep the mass parameter small over many scales. This can be achieved by choosing $\frac{m_\Lambda^2}{\Lambda^2} \approx \frac{h_\Lambda^2}{8\pi^2}$. More concretely speaking, if we want to end up at the scale $\overline{k}$ with a particular mass parameter $\overline{\varepsilon}_{\overline{k}}$ ($u_k := \varepsilon_k \, \tilde{\rho} + \lambda_k \, \tilde{\rho}^2 + ...$), we have to choose

$$\frac{m_\Lambda^2}{\Lambda^2} = \frac{k^2}{\Lambda^2} \overline{\varepsilon}_{\overline{k}} + \frac{h_\Lambda^2}{8\pi^2}. \qquad (6.26)$$

As our numerics should be in perfect agreement with (6.24), we expect that our fine-tuned numerical cut-off mass parameter and the corresponding integrated out mass parameter should fulfill (6.26).

Second, we can see that in the approximation under consideration the ϕ^4 coupling λ_k should flow linearly in $t = \ln \frac{k}{\Lambda}$.

Comparison with numerics Feeding the potential flow equation with a constant Yukawa coupling and a vanishing fermionic anomalous dimension and neglecting the contribution of scalar fluctuations, we run the appropriately fixed binary with a starting potential $u_\Lambda = a\,\rho + 0.5\,\rho^2$ and a large, non-perturbative Yukawa-coupling $h_\Lambda = 10$. We use a non-free starting potential u_Λ for reasons of numerical stability. But we want to stress once more that in this investigation the choice of the cut-off potential does not have an influence on the process of integrating out the fluctuations. We choose a large Yukawa coupling, because then the effects of the fluctuations on the irrelevant operators are best visible. For this setting, we find a stable 'scaling' flow for the choice $a = 0.12...$ (such that the flow passes several scales before it freezes out). The result can be seen in Figure 6.6. We can see immediately that the linear flow of the ϕ^4 coupling is reproduced perfectly, including the slope. We could check the flow of the relevant respectively marginal parameters ε and λ in more detail, but as we are mostly interested in the behaviour of the irrelevant components of the potential, we leave it aside. We only point out that we get indeed very good agreement with (6.26). As the fine-tuning is sensitive to numerical accuracy, we must not expect a priori that we
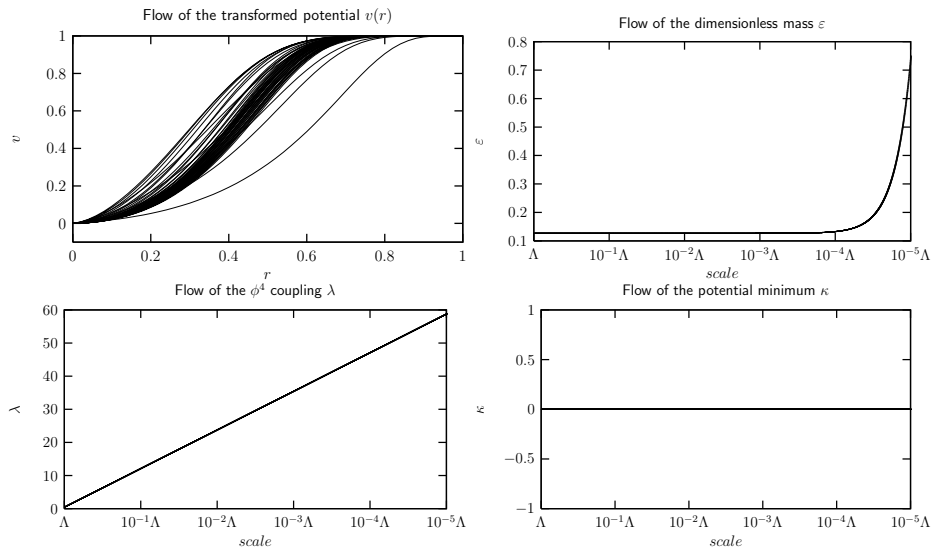
Figure 6.6: Numerical RG flow of the fermionically induced effective average potential in Mean-Field Approximation with starting potential $u_k = 0.12...\tilde{\rho} + 0.5\,\tilde{\rho}^2$ and $h_\Lambda^2 = h_k^2 = 10$.

find the same integrated-out mass parameter, if we feed our analytic solution (6.24) with the numerical cut-off mass parameter. The fact that our numerics is in very good agreement with (6.26) therefore proves that the effects of the limitations of our implementation are negligible. As the mass parameter is the one most sensitive to slight deviations, it is justified to extend this statement to the flow of the potential as a whole. We remark that in the region between four and five integration scales the mass parameter ends to be well fine-tuned, starting its "escape" into the symmetric regime. This means that the theory does not end up with a vacuum expectation value for this particular choice of the cut-off mass parameter.

The analytical prediction of the flow of the potential according to (6.24) with the same cut-off parameters inserted can be seen in Figure 6.7. Now we compare the analytical and the numerical prediction for the potential at three different scales: at $10^{-2}\Lambda, 10^{-4}\Lambda$ and $10^{-5}\Lambda$. We do this by transforming our numerical results, which are given in $v(r)$, back to $u(\rho)$. The superposition can be seen in Figure 6.8. In order to see the importance of the irrelevant operators, we included the purely quadratic part of the analytic solution, i.e. the Taylor expansion up to second order.

64
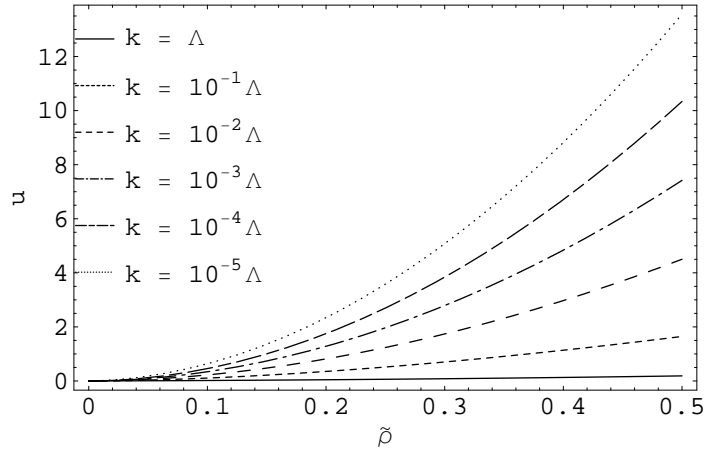
Figure 6.7: Analytical RG flow of the fermionically induced effective average potential in Mean-Field Approximation with starting potential $u_k = 0.12... \, \tilde{\rho} + 0.5 \, \tilde{\rho}^2$ and $h_\Lambda^2 = h_k^2 = 10$.

We see that the analytical and the numerical solution match perfectly! Our approach proves to be able to reproduce the flow of the potential globally. The explicit error given by the discrepancy between the analytical and the numerical solution is depicted on the right hand side in Figure 6.8. The relative error $\Delta u / u$ is of order 10^{-5} and – even more importantly – remains constant in the course of the flow.
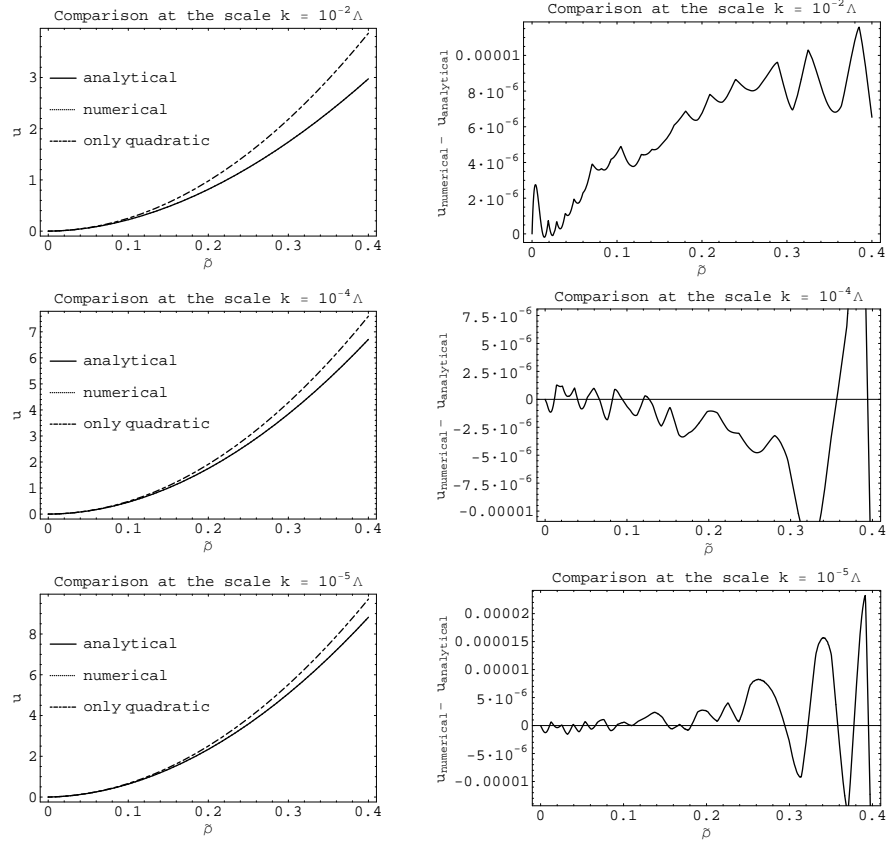
Figure 6.8: Comparison of the analytically and numerically gained fermionically induced effective average potential in Mean-Field Approximation with starting potential $u_k = 0.12...\,\tilde{\rho} + 0.5\,\tilde{\rho}^2$ and $h_\Lambda^2 = h_k^2 = 10$. The plots on the right hand side depict the difference between the numerical and the analytical solution. As can be seen, they are in very good agreement.

Chapter 7

Numerical evaluation

We finally come to the actual issue of this work, the determination of bounds on the Higgs mass in our Toy Model. We show that bounds on the Higgs mass are a direct consequence of the RG flow itself; no further physical or other artificial assumptions have to be imposed. Before we explain our procedure of attaining the bounds, we first demonstrate once more the cause of the seeming instability, which was only briefly sketched in the introduction. We make use of the fermionically induced scalar potential, which was determined in the last chapter. For this simple example, we will give the explicit steps, following Ref. [20]. This makes the occurrence of the seeming instability and its falsity most transparent. After this section we describe the procedure which we follow in order to get the bounds from our numerics. Eventually, we will display our results.

7.1 ...there is no instability!

Starting from the fermionically induced scalar potential (6.23), we derive the seeming instability, which results from using the renormalized potential in regions of σ, where it is not applicable, anymore. We remind the reader that our Toy-SM is considered to be valid only up to a UV cut-off scale Λ. Since we are only interested in the fully integrated-out theory, we first set $k = 0$. Next, we assume $U_\Lambda = \frac{m_\Lambda^2}{2}\,\sigma^2 + \frac{\lambda_\Lambda}{24}\,\sigma^4$, which is convenient, since these are exactly the operators that correspond to counterterms, later on. Thus, we

have

$$U = \frac{m_\Lambda^2}{2}\,\sigma^2 + \frac{\lambda_\Lambda}{24}\,\sigma^4 - \frac{1}{16\,\pi^2}\left[\Lambda^2\,h_\Lambda^2\,\sigma^2 - h_\Lambda^4\,\sigma^4\,\ln\left(\frac{\Lambda^2 + h_\Lambda^2\,\sigma^2}{h_\Lambda^2\sigma^2}\right)\right]. \quad (7.1)$$

We can immediately state that (7.1) is stable over the whole range where it is defined. Note that the particular shape of the potential depends on the chosen regulator, which is in our case a linear cut-off rather than a sharp cut-off. This is of no harm, since the argument only relies on the use of a general momentum space regulator. After expanding the RHS of (7.1) in powers of $\frac{\sigma}{\Lambda}$ and neglecting terms which are suppressed by negative powers of Λ, we get

$$U = \frac{m_\Lambda^2}{2}\,\sigma^2 + \frac{\lambda_\Lambda}{24}\,\sigma^4 - \frac{1}{16\,\pi^2}\left[\Lambda^2\,h_\Lambda^2\,\sigma^2 - h_\Lambda^4\,\sigma^4\,\ln\left(\frac{\Lambda^2}{h_\Lambda^2\,\sigma^2}\right)\right] + \mathcal{O}(\frac{1}{\Lambda^2}).$$

We now move from bare to renormalized perturbation theory by defining

$$\begin{aligned} m_\Lambda^2 &= m_\mu^2 + \delta m^2, \\ \lambda_\Lambda &= \lambda_\mu + \delta\lambda. \end{aligned}$$

We neglect the renormalization of the Yukawa coupling in this simple investigation, $h_\Lambda^2 = h_\mu^2$, since it is irrelevant for the line of argument. We get

$$U = \frac{m_\mu^2}{2}\,\sigma^2 + \frac{\delta m^2}{2}\,\sigma^2 + \frac{\lambda_\mu}{24}\,\sigma^4 + \frac{\delta\lambda}{24}\,\sigma^4 - \frac{1}{16\,\pi^2}\left[\Lambda^2\,h_\mu^2\,\sigma^2 - h_\mu^4\,\sigma^4\,\ln\left(\frac{\Lambda^2}{h_\mu^2\,\sigma^2}\right)\right].$$

The divergent parts of the counterterms thus read

$$\begin{aligned} \delta m^2 &= \frac{\Lambda^2\,h_\mu^2}{8\,\pi^2} + \mathcal{O}(1), \\ \delta\lambda &= \frac{3\,h_\mu^4}{2\,\pi^2}\,\ln\left(\frac{\mu^2}{\Lambda^2}\right) + \mathcal{O}(1), \end{aligned}$$

and we end up with

$$U = \frac{m_\mu^2}{2}\,\sigma^2 + \frac{\lambda_\mu}{24}\,\sigma^4 - \frac{h_\mu^4\,\sigma^4}{16\,\pi^2}\,\ln\left(\frac{h_\mu^2\,\sigma^2}{\mu^2}\right) + \mathcal{O}(1).$$

Since we want to discuss the potential at its minimum, it is convenient to choose the finite parts of δm^2 and $\delta\lambda$ such that the minimum is fixed at its

classical value $v^2 = -\frac{6\,m_v^2}{\lambda_v}$ (Coleman-Weinberg renormalization conditions [29]). We then have

$$U = \frac{m_v^2}{2}\,\sigma^2 + \frac{\lambda_v}{24}\,\sigma^4 - \frac{h_v^4\,\sigma^4}{16\,\pi^2}\left(\ln\frac{\sigma^2}{v^2} - \frac{3}{2}\right) - \frac{h_v^4\,v^2}{8\,\pi^2}\,\sigma^2. \qquad (7.2)$$

(7.2) commonly is believed to be a good approximation as long as

$$\lambda_v \ll 1 \qquad , \qquad h_v \ll 1, \qquad (7.3)$$

and

$$\left|\frac{h_v^4\,\sigma^4}{16\,\pi^2}\,\ln\frac{\sigma^2}{v^2}\right| \ll 1. \qquad (7.4)$$

By choosing λ_v and h_v to fulfill both (7.3) and the additional condition

$$\lambda_v = \frac{3\,h_v^4}{4\,\pi^2}, \qquad (7.5)$$

and considering $\overline{\sigma}$ such that

$$\ln\frac{\overline{\sigma}^2}{v^2} = 2, \qquad (7.6)$$

we find from (7.2) that

$$U(\overline{\sigma}) < U(v).$$

Since $\overline{\sigma}$ fulfills (7.4), one would conclude that (7.2) is still valid at $\overline{\sigma}$ and that we thus have proven the existence of the instability. We now show that this is not the case.

By application of (7.5) and (7.6) one finds that

$$\lambda_v + \frac{3\,h_v^4}{2\,\pi^2}\,\ln\frac{v^2}{\overline{\sigma}^2} < 0.$$

This can be rewritten as inequality for the bare coupling λ_Λ, when remembering that the bare and the renormalized coupling are connected by

$$\lambda_\Lambda = \lambda_v - \frac{3\,h_v^4}{2\,\pi^2}\,\ln\frac{\Lambda^2}{v^2}.$$

We get

$$\lambda_\Lambda + \frac{3\,h_v^4}{2\,\pi^2}\,\ln\frac{\Lambda^2}{\overline{\sigma}^2} < 0. \qquad (7.7)$$

69

But since we have to demand $\lambda_\Lambda > 0$ for the theory to be physically sensible, (7.7) can only be valid for

$$\frac{\Lambda^2}{\overline{\sigma}} \leqslant 1.$$

Thus, $\overline{\sigma}$ has to lie beyond the region of validity of our potential. We conclude that the set of conditions (7.3) and (7.4) is not complete but has to be read together with the constraints $\lambda_\Lambda > 0$ and $\sigma \leqslant \Lambda$. It turns out that this result can be generalized to the stronger statement that the parameter space for renormalized potentials that develop an instability is not connected to the allowed parameter space of bare quantities by a valid RG evolution.

7.2   Attaining the bounds

Our numerics in general is able to determine the flow of our Toy Model truncation for an arbitrarily chosen cut-off potential. Nevertheless, we restrict us to a quartic (dimensionless) starting potential $u_\Lambda(\tilde{\rho}) = \frac{m_\Lambda^2}{\Lambda^2}\tilde{\rho} + \lambda_\Lambda\tilde{\rho}^2$. We will argue later that this indeed does not mean a loss of generality, as long as we are still in the universality class of the Gaussian fixed point. The restriction to a quartic potential allows for a systematic scanning of the bare parameter space. In order to get a non-trivial flow over many scales, we have to fine-tune the starting potential, such that the relevant component is only slightly excited and remains small over several scales. In the vicinity of the Gaussian fixed point, where naive dimensional analysis is valid, the RG direction corresponding to the mass parameter is known to be almost parallel to the relevant eigendirection. It turns out that the mass parameter keeps this property also in non-perturbative regions, at least in our model. We therefore choose it best to be our tuning parameter. As long as the flow is still well fine-tuned, we have the dimensionless potential flow, since then the strong radiative corrections are at least partially compensated by the dimensional flow of the parameters. When the relevant (masslike) component ceases to be fine-tuned and starts to grow exponentially, the radiative corrections become suppressed by the generated mass scales and the dimensional scaling dominates the flow of the parameters. This dimensional running threatens to spoil the numerical flow in dimensionless form. Thus, we switch at the onset of the freeze-out to the fixed-scale flow, which then flows ever less and finally stops. We end up at the integrated-out potential in units of the freeze-out scale. Hence, the flow yields a mapping from the space of the bare param-

eters $m_{k=\Lambda}$, $\lambda_{k=\Lambda}$ (all higher coefficients of the bare potential vanish) and $h_{k=\Lambda}$ onto the space of the renormalized parameters $\breve{u}_{k=0}$ and $h_{k=0}$.

Since we want to mimic the Standard Model, we have to make sure that we only evaluate trajectories that end up at the correct vacuum expectation value and the correct top mass. This yields constraints to the bare parameter space. In addition, we also would wish to control the cut-off Λ. Actually, the constraint on the vacuum expectation value is easy to fulfill: we just demand the freeze-out scale Λ_{fo} to be such that the integrated-out vacuum expectation value v, which our numerics provides in units of the freeze-out scale, comes out correctly. For $\kappa = \frac{1}{2}\, v^2/\Lambda_{\mathrm{fo}}^2$ being the position of the minimum of the integrated-out fixed-scale potential, we have

$$\Lambda_{\mathrm{fo}} = \frac{v}{\sqrt{2\kappa}},$$

where we use the SM value $v = 247$ GeV. Of course, the freeze-out scale is only an auxiliary quantity that mediates the relation between v and Λ. It drops out of the final result and no physical quantity depends on it. By fixing the freeze-out scale, we also determine the cut-off Λ, which follows from

$$\Lambda = 10^{\,diS} \times \Lambda_{\mathrm{fo}},$$

where diS is the number of dimensionless integrated scales. diS is a result of the amount of fine-tuning and thus under our control. But the freeze-out scale, being a result of the overall flow, is no trivial function of the bare paramaters, and therefore can only be determined a posteriori. The same holds for the top mass, which follows from

$$m_t = v\, h.$$

The Yukawa coupling h has to end up at $h = m_t/v = 178\,\mathrm{GeV}/247\,\mathrm{GeV}$ in order to yield the correct top mass. Again, we cannot a priori determine cut-off parameters that guarantee the correct outcome of the Yukawa coupling.

At the end of the day, we want to give the Higgs mass m_H as a function of the bare ϕ^4 coupling λ_Λ for a fixed cut-off Λ and the physical top mass $m_t = 178$ GeV. The Higgs mass is extracted from the flow according to

$$m_H = v\,\sqrt{\breve{u}''(\kappa)},$$

where $\breve{u}''(\kappa)$ is the curvature of the integrated-out fixed-scale potential evaluated at its minimum κ. Since we cannot fix the outcome of the cut-off

and the Yukawa coupling a priori, we follow the strategy to scan the bare parameter space in the vicinity of the bare parameters that would yield the correct top mass and the desired cut-off. If we are sufficiently close to the desired physical parameters, say within a few percent, an interpolation of this data yields a three-dimensional hyper surface in the space spanned by m_t, Λ, λ_Λ and m_H, which we denote by $m_H(\lambda_\Lambda, \Lambda, m_t)$. This interpolating function then can be evaluated at the correct top mass and the desired cut-off, yielding $m_H(\lambda_\Lambda)$. We make this investigation over a wide range of λ_Λ, such that the asymptotic behaviour for $\lambda_\Lambda \to \infty$ and $\lambda_\Lambda \to 0$ can be deduced from our data. This finally yields the striven upper and lower bound to the Higgs mass for a given cut-off Λ.[1]

Does the restriction to a ϕ^4 cut-off potential mean a loss of generality? We want to consider the bounds gained from the procedure outlined above as universally valid, for any arbitrarily chosen cut-off potential. But how can we be sure that there does not exist any complicated non-quartic cut-off potential that bursts our bounds gained from quartic cut-off potentials? The point is that the particular composition of the cut-off potential is not relevant for the outcoming of the flow in the IR, as long as we are still in the universality class of the Gaussian fixed point. The latter is characterized by the existence of exactly one relevant (repulsive) and one marginal eigendirection. The only important properties of the cut-off potential are the excitations of those two components, since all irrelevant directions die out quickly under the flow. Thus, we only have to make sure that our cut-off potential is able to reach any point in this two-dimensional subspace. But this is just achieved by the choice of the quartic starting potential, as long as we can be sure that the overlap of the mass operator and the ϕ^4 operator with the relevant and the marginal direction is still finite. One might argue that the non-quartic operators of an arbitrary cut-off potential should in general modify the IR result. This is surely true for a particular cut-off potential. But we are only interested in the IR results possible at all, no matter from which cut-off potential they emerge. Then, it can be stated that we find for any arbitrary cut-off potential an "equivalent" quartic potential, in the sense that it yields the same IR results. Of course, for a finite cut-off Λ, this holds up to corrections that are supressed by negative powers of Λ. For

---

[1]For a quartic cut-off potential, only positive values of λ_Λ are physically sensible. Hence, it suffices to consider the range of positive ϕ^4 couplings.

instance, if new physics is just around the corner near the electroweak scale $m_{\text{EW}} \lesssim \Lambda$, strongly excited irrelevant directions can substantially modify the Higgs-mass bounds. As a final caveat, let us emphasize that our study so far rests on the assumption that only the Gaussian fixed point is related to a physically relevant universality class. If another universality class potentially connected to a strong-coupling fixed point existed, the conclusions for the validity bounds of the SM could be very different. However, so far we have not discovered any sign of such a universality class.

7.3   Results

We focus on three different scales for the cut-off Λ: $\Lambda = \mathcal{O}(10^6 \, \text{GeV})$, $\Lambda = \mathcal{O}(10^7 \, \text{GeV})$ and $\Lambda = \mathcal{O}(10^8 \, \text{GeV})$. This is an interval in cut-off parameter space, which on the one hand guarantees a sufficiently long flow (in RG "time") to strongly suppress irrelevant directions, and on the other hand is numerically directly accessible by a single fine-tuning procedure. Higher cut-off will require successive fine-tuning, as discussed in Chapter 5. For a fixed bare ϕ^4 coupling λ_Λ, we choose several bare masses and bare Yukawa couplings such that the resulting top masses and cut-offs are in the vicinity of the physical top mass and the considered cut-off, respectively. For the mass parameter in the potential fine-tuning is necessary. We consider a wide range of ϕ^4 couplings over 5 scales, $10^{-3} \leqslant \lambda_\Lambda \leqslant 10^2$. It turns out to be problematic when trying to interpolate the collected data $m_{H,i}(\lambda_{\Lambda,i}, \Lambda_i, m_{t,i})$ in full generality. Thus, we reduce the number of dimensions step by step. First, we project onto the hyper plane defined by the physical top mass by separate interpolation within each subspace of a particular ϕ^4 coupling: $m_{H,j}(\lambda_{\Lambda,\text{fixed}}, \Lambda_j, m_{t,j}) \to m_{H,k}(\lambda_{\Lambda,\text{fixed}}, \Lambda_k, 178 \, \text{GeV})$. Next, we interpolate the resulting data in its Λ dependence, again for each ϕ^4 coupling separately: $m_{H,k}(\lambda_{\Lambda,\text{fixed}}, \Lambda_k, 178 \, \text{GeV}) \to m_H^{\text{approx}}(\lambda_{\Lambda,\text{fixed}}, \Lambda, 178 \, \text{GeV})$. These interpolating functions then can all be evaluated at the same cut-off values; we choose $\Lambda = 3.16 \, 10^6 \, \text{GeV}$, $\Lambda = 3.16 \, 10^7 \, \text{GeV}$ and $\Lambda = 3.16 \, 10^8 \, \text{GeV}$. The resulting plots for the different cut-off scales are displayed in Figure 7.1. One sees immediately the asymptotic behaviour in the limit of vanishing ϕ^4 coupling. The lower bounds to the Higgs mass can be read off directly:
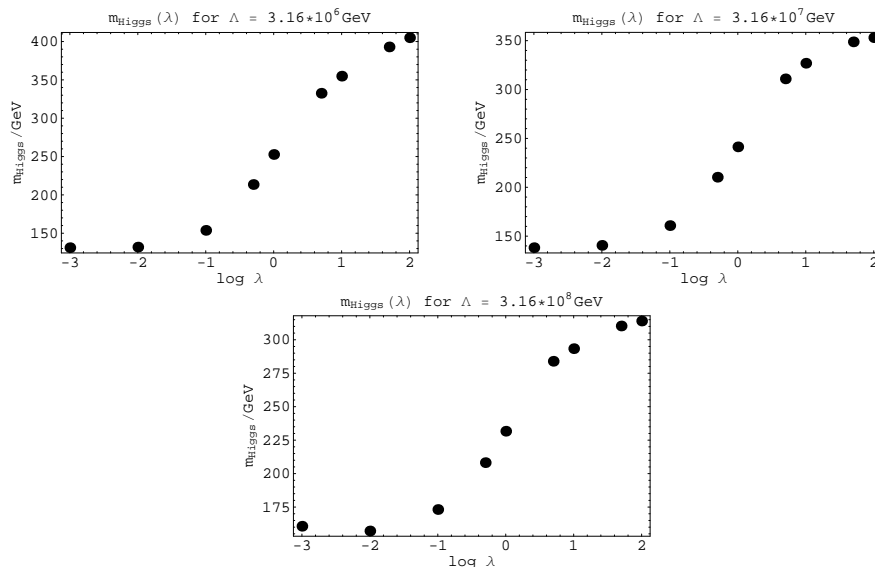
Figure 7.1: The Higgs mass as function of the ϕ^4 coupling for cut-off values $\Lambda = 3.16\,10^6, 3.16\,10^7, 3.16\,10^8$ GeV; the top mass is fixed to its physical value $m_t = 178$ GeV.

Λ	$m_{H,\mathrm{min}}$
$3.16\,10^6$ GeV	131 GeV
$3.16\,10^7$ GeV	138 GeV
$3.16\,10^8$ GeV	157 GeV

For the lower bound at $\Lambda = 3.16\,10^8$ GeV we took the Higgs mass at $\log\lambda = -2$. The slight increase of the Higgs mass at $\log\lambda = -3$ is unexpected; we account it for the numerical inaccuracy of our calculations and use the discrepancy between the two values as error estimate: $\Delta m_{H,\mathrm{min}} \approx 3$ GeV.

The upper bounds we get by extrapolating our data towards arbitrarily large ϕ^4 couplings. We fit the three largest λ values assuming a log-powerlike approach towards the asymptotic value,

$$m_H(\log\lambda) = m_{H,\mathrm{max}} - \frac{a}{\log\lambda} - \frac{b}{(\log\lambda)^2} + \dots,$$

$m_{H,\mathrm{max}}$, a and b being the fitting parameters. We get:

74
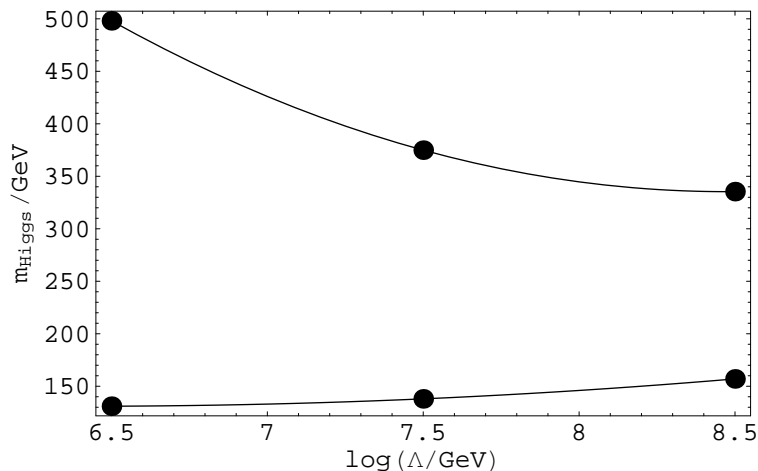
Figure 7.2: Upper and lower bounds to the Higgs mass as function of the cut-off (the interpolating lines are just to guide the eye).

Λ	$m_{H,\max}$
$3.16\,10^6$ GeV	498 GeV
$3.16\,10^7$ GeV	375 GeV
$3.16\,10^8$ GeV	335 GeV

Eventually, we display our final result, the upper and lower bounds to the Higgs mass as functions of the cut-off in the range of our investigation; see Figure 7.2. In view of Figure 7.1 and Figure 7.2, we obviously reached our goal of finding upper and lower bounds to the Higgs mass. The important point is that we did not have to impose any kind of further physical assumptions, as was done in previous investigations of this issue. We showed that the bounds emerge naturally from the RG evolution of the couplings. Unfortunately, so far there are no competing determinations of the Higgs mass bounds in just the same Toy Model; Branchina and Faivre give the bounds following from their criterion based on the inflection point only for the Standard Model itself [20], whereas Holland investigates the Toy Model on the lattice only for $N_F = 8$ fermion flavors [19]. We therefore do not have a base for quantitative comparison, so far. The evaluation of the Toy Model with the competing approaches could be the objective for further investigations. At least, we can state that the qualitative evolution of the bounds with the cut-off meets expectation, which can be seen by comparison with the SM bounds depicted in [19].

Chapter 8

Conclusions and outlook

Let us first summarize our calculations. Motivated by the need for properly deriving upper and lower bounds for the mass of the Higgs particle for a given cut-off, we have investigated a Higgs-Yukawa Toy Model using a functional renormalization group equation. By "boxing" the scalar effective potential and interpolating the transformed potential with Chebyshev polynomials, we have achieved a global description of the potential. Allowing for arbitrary cut-off parameters, but demanding that the IR results yield the correct Standard Model vacuum expectation value and the correct top mass, we find that the RG evolution indeed restricts the possible IR Higgs masses to a finite interval. This finite interval represents the set of renormalized parameters accessible from RG flows which start from all possible relevant and marginal bare parameters. The evolution of the bounds with the cut-off confirms qualitatively and thus justifies the evolution derived for the standard model in previous investigations, which have partly been based on erroneous assumptions.

Unfortunately, a quantitative comparison to competing determinations of the Higgs mass bounds cannot meaningfully be performed at this stage owing to the Toy-model nature of our system. Thus, it should be our most urgent objective to extend our results from the Higgs-Yukawa Toy Model to the Standard Model itself. This can be achieved by including the contributions from the neglected components perturbatively. So far, we can state that, given our Toy Model is a valid approximation to the Standard Model with respect to the qualitative properties of the scalar effective potential, there indeed exist bounds for the SM Higgs mass. In contrast to many earlier studies, these bounds follow from the RG evolution itself and do not

have to rely on additional assumptions, validity bounds of the calculational technique, or unphysical instability scenarios.

Another important point for further investigations, of course, should be to extend the bounds to a wider range in cut-off parameter space. By now, we did not make use of the procedure of successive fine-tuning, as discussed in Chapter 5. Employing this strategy, it would be desirable to get as far as to the Planck scale.

Also, the numerical calculations in this work are exclusively based on the use of linear cut-off functions. Since the approximation of the ERGE causes a regulator dependence of the results, our bounds on the Higgs mass are regulator dependent and thus inherently non-universal. Within the flow equation framework, the regulator dependence can conveniently be studied with the aid of different regulator functions R_k. From optimization considerations, we expect that the present results using the linear regulator mark one extreme of the band of regulator dependencies. The other end may be given by the "sharp" cut-off. Confirming this presumption and determining the resuling error estimate would be desirable.

Our numerical approach is capable to deal with arbitrary cut-off potentials. Nevertheless, our investigation was restricted to quartic cut-off potentials. This was justified by the assumption that our flow is always governed by the Gaussian fixed point. It would be most interesting to check if this assumption is indeed valid for arbitrarily chosen cut-off potentials. The potential discovery of a strong-interaction non-Gaussian fixed point would constitute a new universality class. This could offer a new route to the "triviality" and the hierarchy problem.

Finally, we could investigate cut-off potentials with multiple minima. The non-existence of the instability scenario then should be constructively verifiable by showing the merging of the minima to at most one.

Appendix A

Threshold functions

In this appendix we provide explicit expressions for the threshold integrals introduced in the previous chapters. Our references are [30], [31] and [26].

A.1 General definitions

With the abbreviations

$$
\begin{aligned}
P(q) &= q^2 \left(1 + r_{k,B}(q)\right) \\
P_F(q) &= q^2 \left(1 + r_{k,F}(q)\right)^2 \\
v_d^{-1} &= 2^{d+1}\, \pi^{d/2}\, \Gamma(d/2),
\end{aligned}
$$

the threshold integrals read

$$l_n^d(\omega; \eta_\sigma) = \frac{n + \delta_{n,0}}{4} v_d^{-1} k^{2n-d} \int \frac{d^d q}{(2\pi)^d}$$
$$\times \left\{ \left(\frac{1}{Z_\sigma} \frac{\partial R_k(q)}{\partial t} \right) \left(P(q) + \omega k^2 \right)^{-(n+1)} \right\}$$

$$l_n^{(F)\,d}(\omega; \eta_\psi) = \frac{n + \delta_{n,0}}{2} v_d^{-1} k^{2n-d} \int \frac{d^d q}{(2\pi)^d}$$
$$\times \left\{ \frac{P_F(q)}{1 + r_{k,F}(q)} \left(\frac{1}{Z_{\psi,k}} \frac{\partial \left[Z_{\psi,k} r_{k,F} \right]}{\partial t} \right) \left(P_F(q) + \omega\, k^2 \right)^{-(n+1)} \right\}$$

$$l_{n_1,n_2}^{(FB)\,d}(\omega_1, \omega_2; \eta_\psi, \eta_\sigma) = -\frac{1}{4} v_d^{-1} k^{2(n_1+n_2)-d} \int \frac{d^d q}{(2\pi)^2}$$
$$\times \tilde{\partial}_t \left\{ \frac{1}{\left[P_F(q) + k^2 \omega_1 \right]^{n_1} \left[P(q) + k^2 \omega_2 \right]^{n_2}} \right\}$$

$$m_{n_1,n_2}^d(\omega_1, \omega_2; \eta_\sigma) = -\frac{1}{4} v_d^{-1} k^{2(n_1+n_2-1)-d} \int \frac{d^d q}{(2\pi)^d} q^2$$
$$\times \tilde{\partial}_t \left\{ \frac{\left(\frac{\partial}{\partial q^2} P(q) \right)}{\left[P(q) + k^2 \omega_1 \right]^{n_1}} \frac{\left(\frac{\partial}{\partial q^2} P(q) \right)}{\left[P(q) + k^2 \omega_2 \right]^{n_1}} \right\}$$

$$m_4^{(F)\,d}(\omega; \eta_\sigma) = -\frac{1}{4} v_d^{-1} k^{4-d} \int \frac{d^d q}{(2\pi)^d} q^4$$
$$\times \tilde{\partial}_t \left\{ \frac{\partial}{\partial q^2} \frac{1 + r_{k,F}(q)}{P_F(q) + k^2 \omega} \right\}^2$$

$$m_2^{(F)\,d}(\omega; \eta_\psi) = -\frac{1}{4} v_d^{-1} k^{6-d} \int \frac{d^d q}{(2\pi)^d} q^2$$
$$\times \tilde{\partial}_t \left\{ \frac{\left(\frac{\partial}{\partial q^2} P_F(q) \right)}{\left[P_F(q) + k^2 \omega \right]^2} \right\}^2$$

$$m_{n_1,n_2}^{(FB)\,d}(\omega_1, \omega_2; \eta_\psi, \eta_\sigma) = -\frac{1}{4} v_d^{-1} k^{2(n_1+n_2-1)-d} \int \frac{d^d q}{(2\pi)^d} q^2$$
$$\times \tilde{\partial}_t \left\{ \frac{1 + r_{k,F}(q)}{\left[P_F(q) + k^2 \omega_1 \right]^{n_1}} \frac{\left(\frac{\partial}{\partial q^2} P(q) \right)}{\left[P(q) + k^2 \omega_2 \right]^{n_2}} \right\} .$$

79

A.2   Linear cut-off applied

For the linear cut-off functions

$$r_{k,B}^{lin}(q) = \left(k^2/q^2 - 1\right)\Theta\left(1 - q^2/k^2\right)$$
$$\left(1 + r_{k,B}^{lin}(q)\right) = \left(1 + r_{k,F}^{lin}(q)\right)^2,$$

the integrations can be performed analytically – an enormous advantage for the involved numerics. We obtain

$$l_n^d(\omega;\eta_\sigma) = \frac{2\left(\delta_{n,0} + n\right)}{d}\left(1 - \frac{\eta_\sigma}{d+2}\right)\frac{1}{(1+\omega)^{n+1}}$$

$$l_n^{(F)\,d}(\omega;\eta_\psi) = \frac{2\left(\delta_{n,0} + n\right)}{d}\left(1 - \frac{\eta_\psi}{d+1}\right)\frac{1}{(1+\omega)^{n+1}}$$

$$l_{n_1,n_2}^{(FB)\,d}(\omega_1,\omega_2;\eta_\psi,\eta_\sigma) = \frac{2}{d}\frac{1}{(1+\omega_1)^{n_1}(1+\omega_2)^{n_2}}\times$$
$$\times\left\{\frac{n_1}{1+\omega_1}\left(1 - \frac{\eta_\psi}{d+1}\right) + \frac{n_2}{1+\omega_2}\left(1 - \frac{\eta_\sigma}{d+2}\right)\right\}$$

$$m_{n_1,n_2}^d(\omega_1,\omega_2;\eta_\sigma) = \frac{1}{(1+\omega_1)^{n_1}(1+\omega_2)^{n_2}}$$

$$m_4^{(F)\,d}(\omega;\eta_\psi) = \frac{1}{(1+\omega)^4} + \frac{1-\eta_\psi}{d-2}\frac{1}{(1+\omega)^3}$$
$$-\left(\frac{1-\eta_\psi}{2\,d-4} + \frac{1}{4}\right)\frac{1}{(1+\omega)^2}$$

$$m_2^{(F)\,d}(\omega;\eta_\psi) = \frac{1}{(1+\omega)^4}$$

$$m_{n_1,n_2}^{(FB)\,d}(\omega_1,\omega_2;\eta_\psi,\eta_\sigma) = \left(1 - \frac{\eta_\sigma}{d+1}\right)\frac{1}{(1+\omega_1)^{n_1}(1+\omega_2)^{n_2}}\,.$$

Appendix B

Transformed potential flow equation

We apply our 'boxing' transformation rules (5.1) and (5.2) to the flow equation for the potential (4.11). This yields

$$
\begin{aligned}
\partial_t v_k &= -d\,(1 - v_k^2)\,\mathrm{arctanh}\,v_k - (d - 2 + \eta_\sigma)\,(1 - r)\,\ln(1 - r)\,v_k' \\
&\quad + 2\,v_d\,\alpha\,(1 - v_k^2)\left[l_0^d(\omega_1; \eta_\sigma) - d_\gamma\,l_0^{(F)d}(\omega_2; \eta_\psi)\right] \\
&\quad - 2 v_d\,\alpha\,(1 - v_k^2)\left[l_0^d(\omega_3; \eta_\sigma) - d_\gamma\,l_0^{(F)d}(0; \eta_\psi)\right],
\end{aligned}
$$

with

$$
\begin{aligned}
\omega_1 &= \frac{(1 - r)\,v_k'\,\beta}{\alpha\,(1 - v_k^2)} - \frac{4\,v_k\,\beta\,(1 - r)^2\,\ln(1 - r)\,v_k'^2}{\alpha\,(1 - v_k^2)^2} \\
&\quad + \frac{2\,\beta\,(1 - r)\,\ln(1 - r)\,v_k'}{\alpha\,(1 - v_k^2)} - \frac{2\,\beta\,(1 - r)^2\,\ln(1 - r)\,v_k''}{\alpha\,(1 - v_k^2)} \\
\omega_2 &= -\frac{2}{\beta}\,h_k^2\,\ln(1 - r) \\
\omega_3 &= \frac{\beta\,v_k'(0)}{\alpha\left(1 - v_k^2(0)\right)},
\end{aligned}
$$

where the primes denote derivatives with respect to r.

81

Appendix C

Chebyshev polynomials

We give a short introduction into definition and fundamental properties of the Chebyshev polynomials. Our reference is [32].

The Chebyshev polynomials $T_n(x)$ can be defined as the set of polynomials being orthogonal in the interval [-1,1] over the weight $(1 - x^2)^{-1/2}$:

$$\int_{-1}^{1} \frac{T_i(x)T_j(x)}{\sqrt{1 - x^2}} = \left\{ \begin{array}{ll} 0 & i \neq j \\ \pi/2 & i = j \neq 0 \\ \pi & i = j = 0 \end{array} \right. .$$

They are given by the explicit formula

$$T_n(x) = \cos(n \arccos x),$$

which yields for the first few polynomials

$$\begin{array}{rcl} T_0(x) & = & 1 \\ T_1(x) & = & x \\ T_2(x) & = & 2x^2 - 1 \\ T_3(x) & = & 4x^3 - 3x \\ T_4(x) & = & 8x^4 - 8x^2 + 1. \\ & \vdots & \end{array}$$

The polynomial $T_n(x)$ has n zeros in the interval [-1,1], and they are located at the points

$$x = \cos\left(\frac{\pi(k - \frac{1}{2})}{n}\right) \qquad k = 1, 2, ..., n.$$

The Chebyshev approximation of some arbitrary function $f(x)$ in the interval [-1,1] is given by

$$f(x) \approx \left[\sum_{k=0}^{N-1} c_k T_k(x) \right] - \frac{1}{2} c_0,$$

where the N coefficients are defined by

$$
\begin{aligned}
c_j &= \frac{2}{N} \sum_{k=1}^{N} f(x_k) T_j(x_k) \\
&= \frac{2}{N} \sum_{k=1}^{N} f\left[\cos\left(\frac{\pi(k - \frac{1}{2})}{N} \right) \right] \cos\left(\frac{\pi j(k - \frac{1}{2})}{N} \right).
\end{aligned}
$$

Note that these coefficients are attained by evaluating $f(x)$ at the zeros of the N'th Chebyshev polynomial.

Bibliography

[1] M. Luscher and P. Weisz, Nucl. Phys. **B295**, 65 (1988).

[2] M. Gockeler *et al.*, Phys. Rev. Lett. **80**, 4119 (1998), hep-th/9712244.

[3] H. Gies and J. Jaeckel, Phys. Rev. Lett. **93**, 110405 (2004), hep-ph/0405183.

[4] H. Gies, J. Jaeckel, and C. Wetterich, Phys. Rev. **D69**, 105008 (2004), hep-ph/0312034.

[5] T. Hambye and K. Riesselmann, (1997), hep-ph/9708416.

[6] M. Sher, Phys. Rept. **179**, 273 (1989).

[7] M. Lindner, Zeit. Phys. **C31**, 295 (1986).

[8] N. V. Krasnikov, Yad. Fiz. **28**, 549 (1978).

[9] P. Q. Hung, Phys. Rev. Lett. **42**, 873 (1979).

[10] H. D. Politzer and S. Wolfram, Phys. Lett. **B82**, 242 (1979).

[11] N. Cabibbo, L. Maiani, G. Parisi, and R. Petronzio, Nucl. Phys. **B158**, 295 (1979).

[12] R. A. Flores and M. Sher, Phys. Rev. **D27**, 1679 (1983).

[13] C. Ford, D. R. T. Jones, P. W. Stephenson, and M. B. Einhorn, Nucl. Phys. **B395**, 17 (1993), hep-lat/9210033.

[14] M. Sher, Phys. Lett. **B317**, 159 (1993), hep-ph/9307342.

[15] G. Altarelli and G. Isidori, Phys. Lett. **B337**, 141 (1994).

84

[16] J. A. Casas, J. R. Espinosa, and M. Quiros, Phys. Lett. **B342**, 171 (1995), hep-ph/9409458.

[17] J. A. Casas, J. R. Espinosa, and M. Quiros, Phys. Lett. **B382**, 374 (1996), hep-ph/9603227.

[18] G. Isidori, G. Ridolfi, and A. Strumia, Nucl. Phys. **B609**, 387 (2001), hep-ph/0104016.

[19] K. Holland, Nucl. Phys. Proc. Suppl. **140**, 155 (2005), hep-lat/0409112.

[20] V. Branchina and H. Faivre, Phys. Rev. **D72**, 065017 (2005), hep-th/0503188.

[21] K. G. Wilson and J. B. Kogut, Phys. Rept. **12**, 75 (1974).

[22] F. J. Wegner and A. Houghton, Phys. Rev. **A8**, 401 (1973).

[23] C. Wetterich, Phys. Lett. **B301**, 90 (1993).

[24] N. Tetradis and C. Wetterich, Nucl. Phys. **B422**, 541 (1994), hep-ph/9308214.

[25] D. Litim, Nucl. Phys. **B631**, 128 (2002), hep-th/0203006.

[26] F. Hoefling, C. Nowak, and C. Wetterich, Phys. Rev. **B66** (2002), cond-mat/0203588.

[27] K. Wilson and M. Fisher, Phys. Rev. Lett. **28**, 240 (1972).

[28] M. E. Peskin and D. V. Schroeder, *An Introduction to quantum field theory* , Reading, USA: Addison-Wesley (1995) 842 p.

[29] S. R. Coleman and E. Weinberg, Phys. Rev. **D7**, 1888 (1973).

[30] D.-U. Jungnickel and C. Wetterich, Phys. Rev. **D53**, 5142 (1996), hep-ph/9505267.

[31] J. Berges, N. Tetradis, and C. Wetterich, Phys. Rept. **363**, 223 (2002), hep-ph/0005122.

[32] W. H. Press, S. A. Teukolsky, W. T. Vettering, and B. P. Flannery, *Numerical Recipes* , Cambridge University Press.

Danke!

Erklärung:

Ich versichere, dass ich diese Arbeit selbständig verfasst und keine anderen als die angegebenen Quellen und Hilfsmittel benutzt habe.

Heidelberg, den 22. März 2011   . . . .
                                                            Unterschrift